Physikalisch-Technische Bundesanstalt

PTB-Bericht

PTB-Dos-13

April 1986

J. Böhm

The National Primary Standard of the PTB for Realizing the Unit of the Absorbed Dose Rate to Tissue for Beta Radiation

ISSN 0172-7095

PTB

Recommended citation format:
Böhm, Jürgen. The National Primary Standard of the PTB for Realizing the Unit of the Absorbed Rate to Tissue for Beta Radiation. Physikalisch-Technische Bundesanstalt (PTB), 1986.
Available by: https://doi.org/10.7795/110.20190315A

P H Y S I K A L I S C H - T E C H N I S C H E B U N D E S A N S T A L T

Gruppe Strahlenschutzmetrologie

Bericht Dos-13

THE NATIONAL PRIMARY STANDARD OF THE PTB FOR REALIZING THE UNIT OF THE ABSORBED DOSE RATE TO TISSUE FOR BETA RADIATION *)

by

Jürgen Böhm

Braunschweig, April 1986

ISSN 0172-7095

*) Dedicated to Prof. Dr. W. Kolb on the occasion of his 60th birthday.

Verfügbar unter: https://doi.org/ 10.7795/110.20190315A

Abstract

The national primary standard of the PTB with its extrapolation chambers and associated equipment is described. The evaluation procedure including all the corrections of the measured values is discussed in detail. Measurement uncertainties are stated for beta ray sources of the radionuclides (^{90}Sr + ^{90}Y), ^{204}Tl, and ^{147}Pm. An intercomparison with the NPL of beta ray sources of these radionuclides shows that the results agree within the uncertainties claimed.

Zusammenfassung

Die nationale Primärnormal-Meßeinrichtung der PTB mit ihren Extapolationskammern und zugehörigen Meßgeräten wird beschrieben. Auf das Auswerteverfahren einschließlich aller Korrektionen wird ausführlich eingegangen. Meßunsicherheiten werden für Betastrahler der Radionuklide (^{90}Sr + ^{90}Y), ^{204}Tl und ^{147}Pm angegeben. Vergleichsmessungen mit dem NPL, durchgeführt mit Betastrahlern dieser Radionuklide, liefern Ergebnisse, die innerhalb der angegebenen Meßunsicherheiten übereinstimmen.

Contents

1 INTRODUCTION

According to the German Units Act /1/ the Physikalisch-Technische Bundesanstalt must define and publish procedures for realizing unembodied units such as the Gray per second (Gy s^{-1}) for the absorbed dose rate to tissue produced by beta radiation. The product of the absorbed dose rate and a quality factor (the quality factor is unity for beta radiation) is defined as the dose equivalent rate in the "Ordinance on Protection against Damage and Injuries caused by Ionizing Radiation" /2/. This ordinance contains a number of limiting values for body doses, i.e. dose equivalents, and in some cases prescribes the observance of these limiting values by measurements.

The realization and dissemination of the unit Gy s^{-1} for beta radiation comprises

- the generation of known fields of beta radiation (reference fields),
- the development and improvement of primary standards (extrapolation chambers and associated equipment) and their comparison with similar devices of other countries, and
- the calibration of secondary standards, dose equivalent and dose equivalent rate meters.

Beta sources containing the radionuclides (^{90}Sr + ^{90}Y), ^{204}Tl and ^{147}Pm are used to produce reference fields (see table 1). The sources are usually used together with beam flattening filters specified in the international standard ISO 6980 /3/ to ensure that the characteristics of the fields comply with this standard. Areas up to 15 cm in diameter of uniform dose rate are produced by means of the beam flattening filters, enabling relatively large beta dosemeters to be calibrated. The

Table 1: Types of beta ray sources which are used to produce reference fields and for which data are shown in this report at the specified calibration distances.

	Source type				
	1	2	3	4	5
Radionuclide	^{147}Pm	^{204}Tl	$^{90}Sr + ^{90}Y$	$^{90}Sr + ^{90}Y$	$^{90}Sr + ^{90}Y$
Mass per area of the inactive silver foil "window" in mg cm^{-2}	5 ± 1	20 ± 3	50 ± 5	50 ± 5	50 ± 5
Protection against corrosion	0.5 mg cm^{-2} electroplating of nickel	1 µm thin gold flashing	1 µm thin gold flashing	0.1 mm stainless steel	0.1 mm stainless steel
Mean beta ray energy in MeV	0.06	0.24	0.8	0.8	0.8
Filter according to ISO 6980	yes	yes	yes	yes	no
Calibration distance in cm	20	30	30	30	11; 30; 50

range of the mean energies of the beta rays is 0.06 MeV to 0.8 MeV, the range of the absorbed dose rates about 1 nGy s^{-1} to 1 mGy s^{-1}.

Calibrations of beta sources, dose equivalent and dose equivalent rate meters have been reported /4-9/. The beta sources sent to the PTB for calibration differed in their relative spectral flux densities and angular distributions of the beta particles. The calibration of these sources turned out to be time consuming and expensive because of the numerous measurements needed. On the initiative of some users the secondary standard for the absorbed dose rate for beta radiation developed in the National Physical Laboratory /10,11/ was modified and the prototype was offered to industry for manufacture under licence /12,13/. As the relative spectral flux densities of the same types of beta sources contained in the secondary standard agree well, many time consuming measurements, for example the determination of the correction factors k_{ab} and k_{pe} (see section 5), need to be performed only once. The other sources need be measured only relative to the first ones. Up to now 65 secondary standards have been calibrated in the PTB and are here referred to as "PTB secondary standards".

Sources of types 1 to 3 (table 1) are constituents of all NPL secondary standards and of the PTB secondary standards 1 to 23. Sources of type 3 are replaced in the PTB secondary standards 24 to 65 by those of type 4 with a thicker encapsulation (0.1 mm stainless steel) to avoid leakage of radioactive material. Every PTB secondary standard contains a type 5 source of high activity (about 1.9 GBq) calibrated without any beam flattening filter.

Two types of extrapolation chambers are used for the measurements of the absorbed dose rates: one with a very low leakage current but with a re-

latively high polarity effect for the measurement of the absorbed dose rates below about 10 μGy s^{-1}, the other with a higher leakage current but with a small polarity effect for the higher absorbed dose rates. The latter has been proved capable of also measuring soft X-rays /14/. The extrapolation chambers and their associated equipment have been compared with other standards /4,6,15-17/.

This paper contains the description of the national primary standard and the procedure for determining the absorbed dose rate to tissue. The component uncertainties contributing to the overall uncertainty of the absorbed dose rate are discussed for measurements of sources containing the radionuclides (^{90}Sr + ^{90}Y), ^{204}Tl, and ^{147}Pm. The results of an intercomparison with the NPL of sources of these radionuclides are reported.

2 MEASURAND *)

The quantity to be determined by the primary standard is the absorbed dose rate $\dot{D}_t(0)$ **) to tissue on the surface of a semi-infinitely extended phantom of tissue. Tissue is the short form for tissue equivalent material with the composition related to mass of 76.2 % O, 10.1 % H, 11.1 % C and 2.6 % N /18/. Its density is 1 g cm^{-3}.

---

*) The word "measurand" was introduced by /44/ to designate the quantity to be measured.

**) The symbol $\dot{D}_t(0)$ corresponds to the symbol $\dot{D}_g(0)$ in the PTB calibration certificates of the secondary standards (Index "t" for tissue and Index "g" for the German "Gewebe"). The number in brackets, later also used together with $\dot{H}'$, is the depth x in mm below the surface of the phantom.

The unit of $\dot{D}_t(0)$ is J kg^{-1} s^{-1}, the special name for this being gray per second (Gy s^{-1}).

$$1 \text{ Gy } s^{-1} = 1 \text{ J } kg^{-1} s^{-1} \qquad (1)$$

The absorbed dose rate to tissue, $\dot{D}_t$, is closely related to the quantity dose equivalent rate, $\dot{H}$, used in radiation protection which is given for beta radiation by

$$\dot{H} = q \dot{D}_t \qquad (2)$$

with q = 1 Sv Gy^{-1}.
The quotient $\dot{D}_t(x)/\dot{D}_t(0)$ is called the transmission factor T'(x).

The quantities "directional dose equivalent rate", $\dot{H}'(0.07)$ and $\dot{H}'(10)$, are defined in a 30 cm diameter sphere of tissue /19/ and can be calculated in good approximation from $\dot{D}_t(0.07)$ and $\dot{D}_t(10)$, as the different geometries related to the quantities (sphere and semi-infinitely extended slab phantom) are of no practical influence in the case of beta radiation:

$$\dot{H}'(0.07) = q \dot{D}_t(0.07), \qquad (3)$$

$$\dot{H}'(10) = q \dot{D}_t(10). \qquad (4)$$

3 PRIMARY STANDARD

3.1 EXPERIMENTAL ARRANGEMENT

A schematic diagram of the experimental arrangement is shown in figure 1. The current produced by an extrapolation chamber (details see section 3.2) irradiated by beta radiation is measured by means of a vibrating capacitor amplifier (Cary Model 401) with capacitive feedback. The amplifier enables measurements of currents down to 10 fA to be carried out

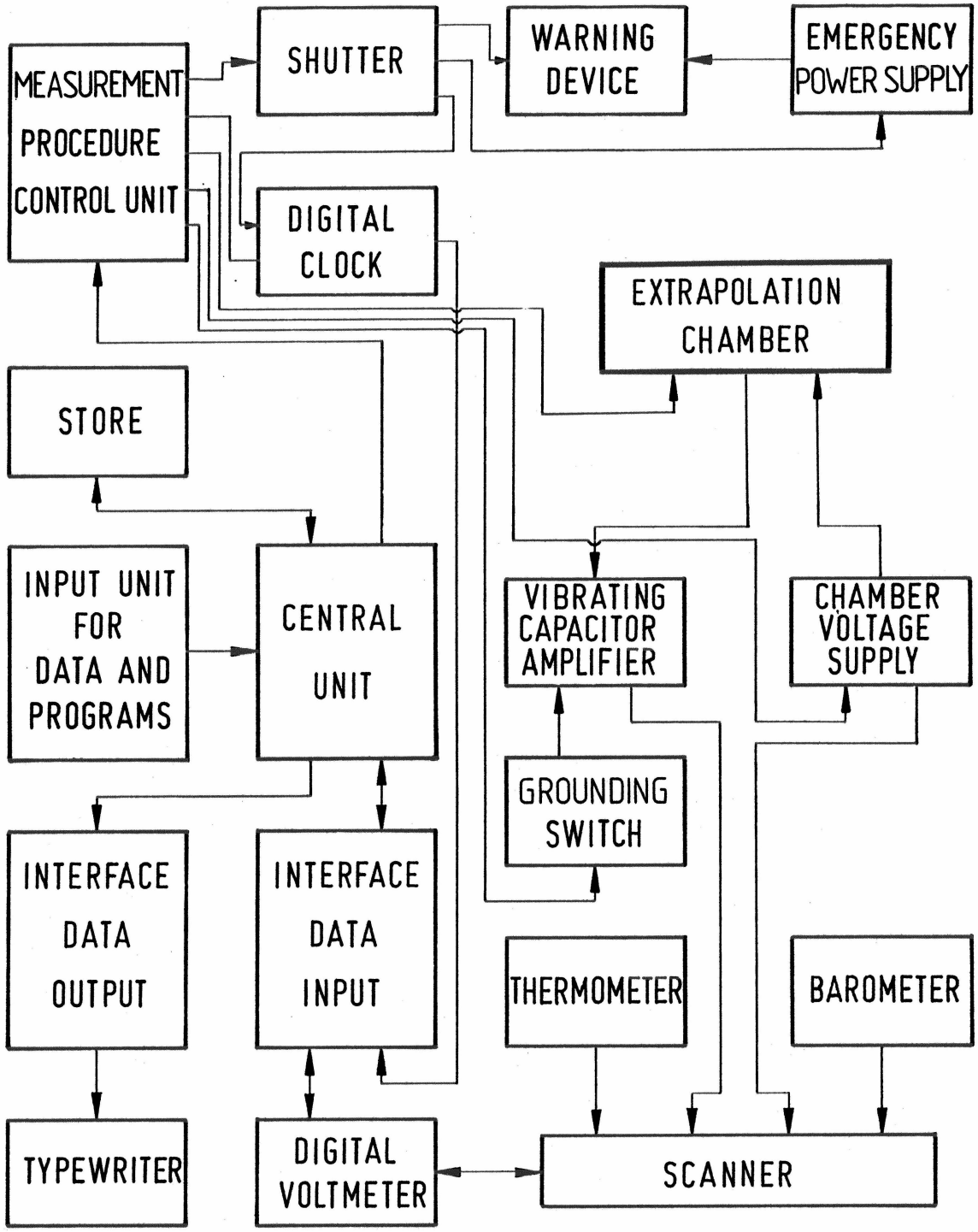

Figure 1: Schematic diagram of the experimental arrangement of the primary standard.

with a relative standard deviation for a single measurement of 0.1 % to 0.2 % and a relative systematic uncertainty of 0.05 % /20/. The amplifier can be grounded by remote control. Its output voltage is fed into a scanner.

The extrapolation chamber is connected to a programmable voltage supply. The chamber depth is changed by a small remote-controlled motor coupled to the micrometer screw of the extrapolation chamber. The chamber depth is measured with a sealed, incremental transducer (Heidenhain Model 3010) connected to the measurement procedure control unit (Hewlett Packard Model 9810). The indications of the incremental transducer and the micrometer screw differed by less than 1 µm.

The temperature and relative humidity of the air in the collecting volume of the extrapolation chamber and between the extrapolation chamber and the beta source are stabilized by air conditioning to (20 ± 0.2) °C and (45 ± 10) %, respectively. The air pressure varies due to atmospheric conditions around about 100 kPa. The electric signals from a thermometer and a barometer are fed into the scanner.

The central unit (Hewlett-Packard Model 9810) controls the whole measurement cycle: Setting of the depth and voltage of the extrapolation chamber; reading and printing of the output voltage of the vibrating capacitor amplifier and the devices for measuring the air temperature and pressure after a preset time; zero setting of the vibrating capacitor amplifier; restarting of the cycle. Thus the measurement of an extrapolation curve (see section 4) can be performed automatically.

3.2 EXTRAPOLATION CHAMBER

3.2.1 General

The extrapolation chamber serves to realize a small air-filled ionization volume with a variable mass m_a of air at a point of interest in a phantom. The ionization volume approximates part of a small air slice in the phantom /21/. The extrapolation chamber is so constructed that the measurement of the increment of the ionization current (corrected for recombination losses), ΔI, per increment of the air mass of the collecting volume, Δm_a, is performed as close as possible under Bragg-Gray conditions (BGC) /22,23/. Minor deviations from the Bragg-Gray conditions are expected to be eliminated by extrapolating $\Delta I/\Delta m_a$ towards zero chamber depth:

$$\dot{D}_t = s_{t,a} \frac{W}{e} \left(\frac{\Delta I}{\Delta m_a}\right)_{BGC} \qquad (5)$$

where $s_{t,a}$ is the ratio of the average mass collision stopping powers for tissue and air averaged over the spectral beta particle flux density;

W the average energy required to produce an ion pair in air;

e the elementary charge;

$\left(\frac{\Delta I}{\Delta m_a}\right)_{BGC}$ the limiting value of the quotient of the increment of the ionization current, ΔI, per increment of the mass of the chamber gas, Δm_a, obtained for Bragg-Gray conditions (BGC).

The determination of the quotient $(\Delta I/\Delta m_a)$ for Bragg-Gray conditions can be interpreted as the determination of the ionization current (corrected for saturation) ΔI from a hypothetical chamber with the air mass Δm_a operated under Bragg-Gray conditions. In contrast to other dosimetric measuring methods with ionization chambers, here the exact value of the chamber depth itself need not be known, only its change.

3.2.2 Construction

The cross section of the extrapolation chambers used is shown schematically in figure 2. All parts of the chamber hit by beta rays (from the left) are made of polymethylmethacrylate ("Plexiglas", perspex), polyethylene terephthalate film ("Hostaphan", mylar), and carbon which are in good approximation equivalent to tissue with respect to the transmission and backscattering of beta rays. The entrance window (7) is a graphite-coated "Hostaphan" foil, the foil thickness without coating being 3.5 µm. The foil is stretched by a ring (4) on the electrode housing (3) made of perspex. The entrance foil (7) is connected to the collecting potential via the socket (2). There are two types of counter-electrodes which contain the collecting electrode (6).

The first type (for more details see figure 3a) consists of a perspex block (5) 60 mm in diameter and 31 mm in depth with a graphited surface (6), which is divided into a circular collecting electrode 30 mm in diameter, and a guard ring. Both areas are separated by a groove which is 0.2 mm in width and depth. A carbon wire 0.1 mm thick connects the collecting electrode to the socket (8).

The second type (see figure 3b) consists of a graphite block 60 mm in diameter and 20 mm in depth which is covered by a 0.5 mm thick layer of

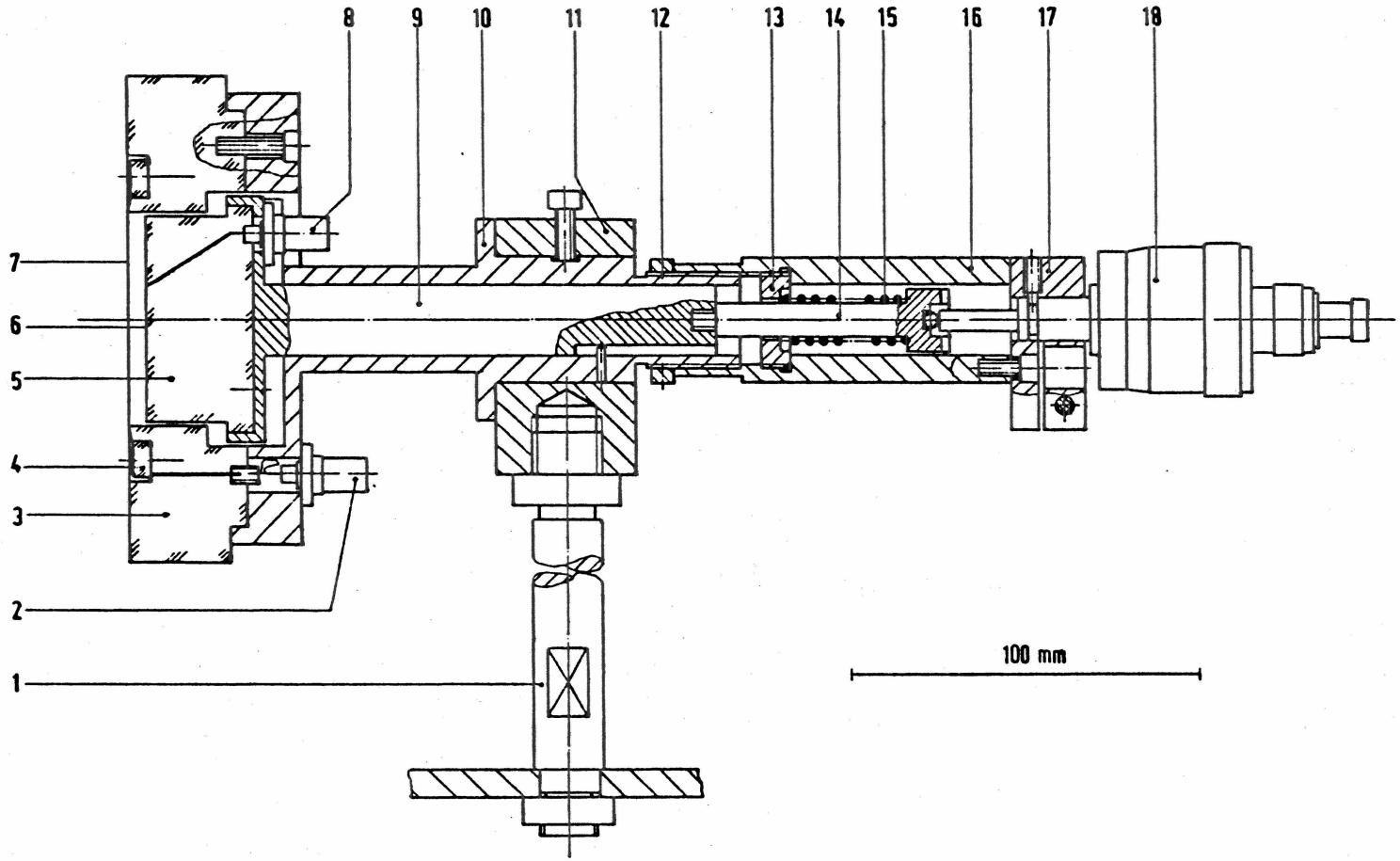

Figure 2: Extrapolation chamber of type 1. Explanations: 1. Stand; 2. Socket for collecting voltage; 3. Housing of perspex; 4. Tension ring; 5. Perspex block; 6. Graphited surface divided into collecting electrode and guard ring; 7. Entrance foil; 8. Socket for collecting electrode; 9. Sliding-fit rod; 10. Cylindrical guide for rod 9; 11. Holder; 12. Adjustable nut; 13. Threaded ring; 14. Bolt; 15. Spring; 16. Tube; 17. Clamping piece; 18. Micrometer screw.

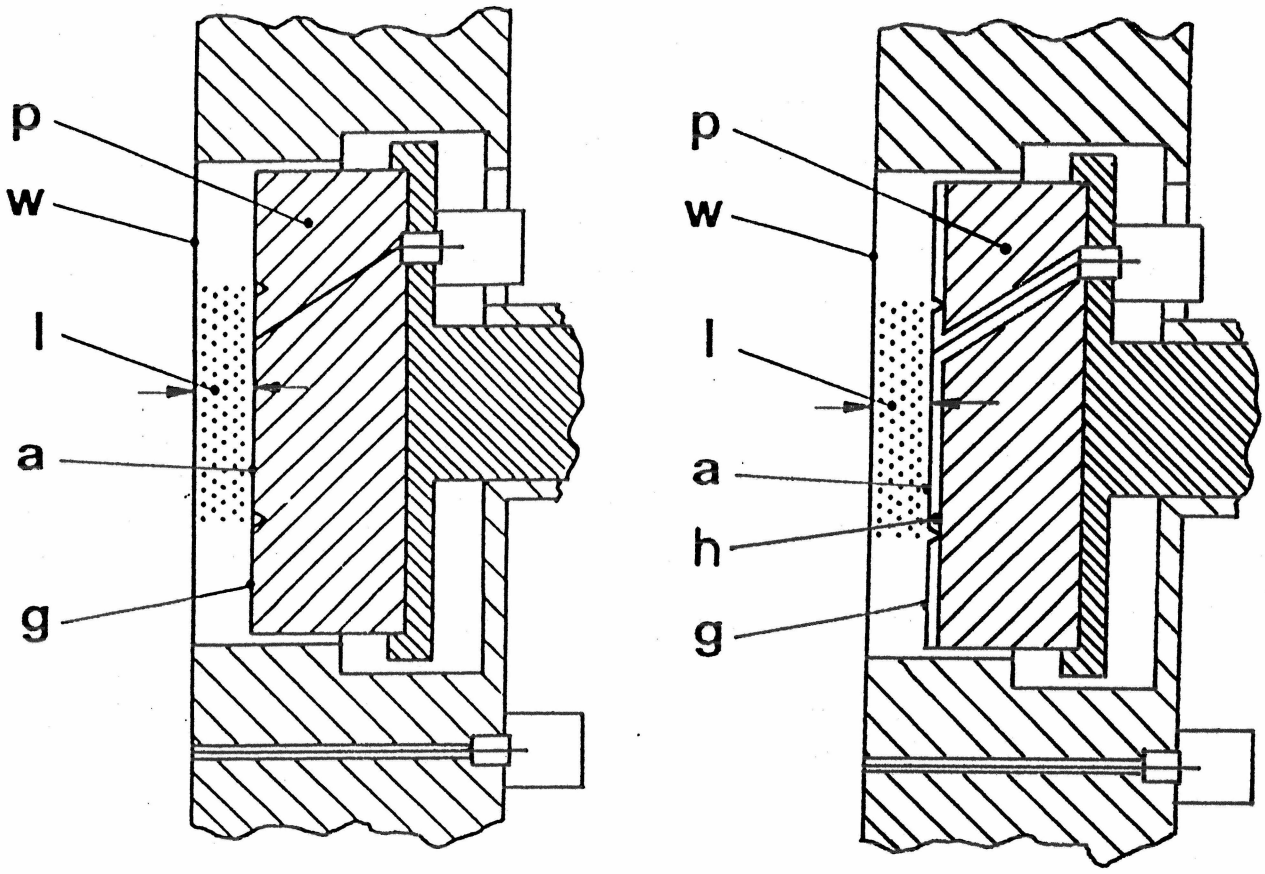

(a) (b)

Figure 3: Schematic cross sections of the main parts of the extrapolation chamber of type 1 (figure (a)) and type 2 (figure (b)). The collecting volume is indicated by the dotted area. Explanations:

p piston made of perspex (figure (a)) or graphite (figure (b));

w entrance window;

l chamber depth;

a area of collecting electrode;

g guard ring;

h thin perspex layer (figure (b)).

perspex. As with the first type, the surface of the perspex layer is graphited and divided into a circular collecting electrode and a guard ring. A copper wire 0.1 mm thick surrounded by about 2 mm of perspex connects the collecting electrode to the socket. In the following the two extrapolation chambers differing in the construction of the electrode are referred to as types 1 and 2.

The depth of the measuring volume of the extrapolation chamber can be changed by varying the distance between the electrodes (6) and (7) in the range of 0 to 10.5 mm. The chamber was designed taking into consideration the fact that the change in the distance between the electrodes can be performed with an uncertainty below 1 µm, whereby the parallelism of the electrodes is maintained. This was made possible by mounting the piston with the collecting electrode on a sliding-fit rod (9) which is movable by means of a spring (15) in a 125 mm long cylindrical guide for the rod. The guide (10) is longer than that commonly used in comparable chamber constructions and this led to a relatively long chamber, but this guide length was found to be necessary to minimize the tilt of the rod (9) in the guide (10). The chamber depth can be varied by a micrometer screw (18) coupled to a bolt (14) screwed into the rod (9). The micrometer screw (18) is adjustable by means of the clamping piece (17), the tube (16), the threaded ring (13) and the nut (12) so that its indication exactly fits the actual chamber depth and the scale is turned towards the observer. A small motor for remote-control turning of the micrometer screw and a remote-controlled incremental transducer for measuring the chamber depth were added at a later stage of the chamber's operation and are not shown in figure 2. The chamber is screwed onto the measuring table by means of the holder (11) and the stand (1).

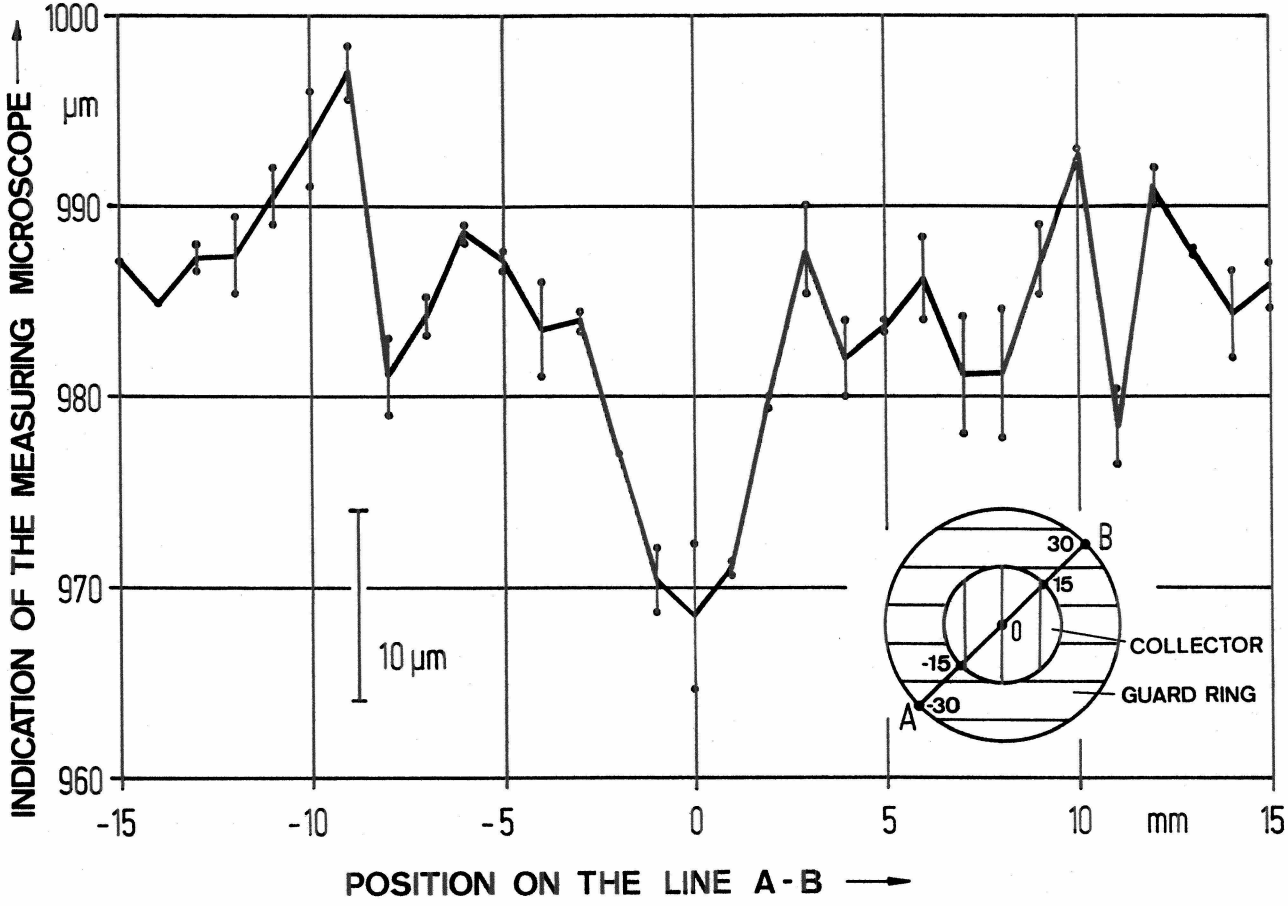

Figure 4: Measurements of the unevenness of the collector of the type 1 extrapolation chamber obtained by means of a measuring microscope.

Before graphiting the perspex block (5) of the type 1 extrapolation chamber, the unevenness of its surface was measured by a special microscope. The result is shown in figure 4. The grooves are due to machining on the lathe. In order to avoid larger dent depressions the surface was not polished after machining. The surface proved to be sufficiently flat for the measurements.

4 EVALUATION OF THE MEASUREMENTS

To obtain the absorbed dose rate $\dot{D}_t(0)$ the factors on the right of eq.(5) must be determined, whereby the quotient $(\Delta I)/(\Delta m_a)_{BGC}$ is usually most difficult to obtain. If the measurements with the extrapolation chamber were performed under Bragg-Gray conditions, this quotient could be simply obtained from the slope of the extrapolation curve (plot of I versus chamber depth L) divided by the chamber gas density and the effective collector area. Unfortunately, Bragg-Gray conditions are always more or less violated which can be seen from the extrapolation curves for the sources of types 1 to 3 (table 1) in figure 5: the slope of the extrapolation curve varies with chamber depth.

To overcome these difficulties, all available corrections for achieving Bragg-Gray conditions should be applied, possibly by means of additional measurements. Moreover, it is recommended that the slope of the extrapolation curve versus chamber depth L be plotted and the slope towards $L = 0$ extrapolated. This procedure has been discussed in more detail for soft X-rays elsewhere /14/. Eq. (5) can be written as follows if every correction is formally considered by a correction factor:

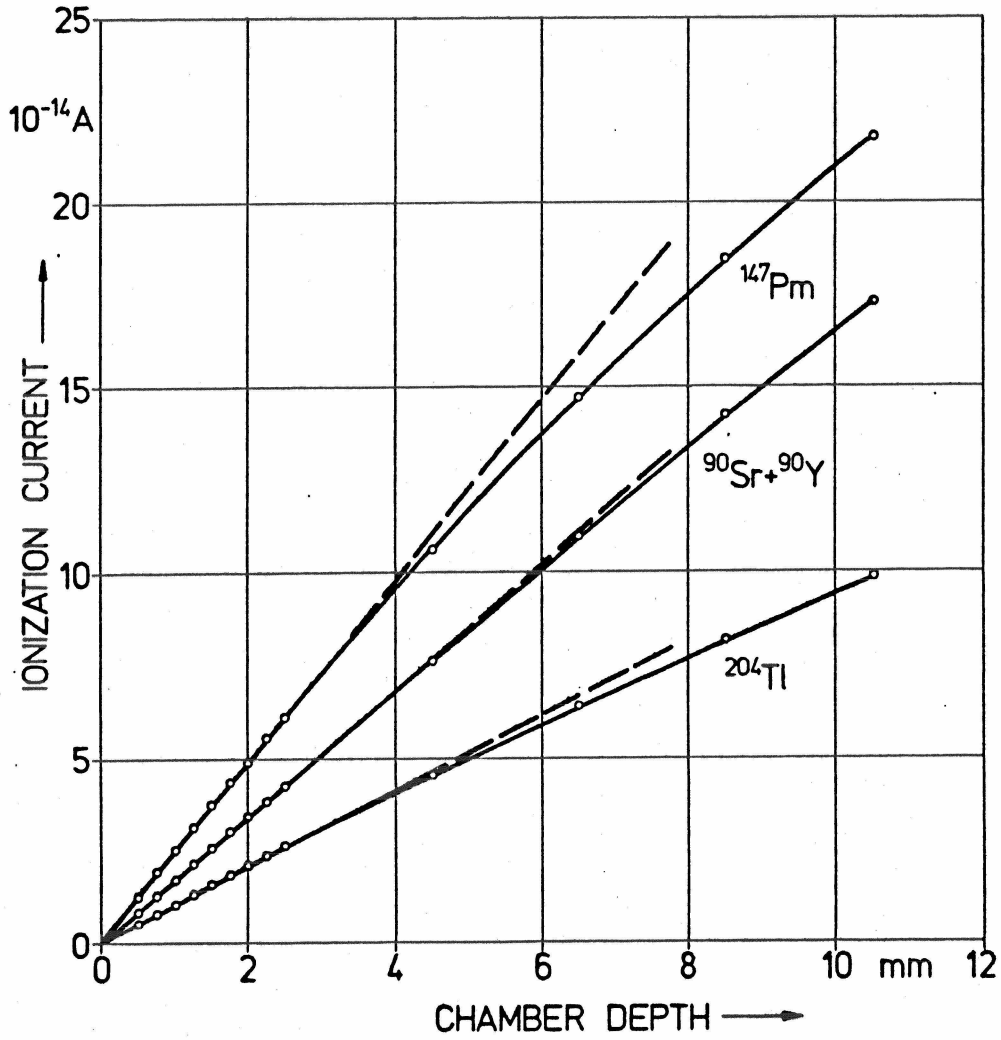

Figure 5: Extrapolation curves of the sources of types 1 to 3 (see table 1) measured with the type 1 extrapolation chamber. The ionization current $(I_+ - I_-)/2$ (see section 5.5) is plotted versus the chamber depth. The dashed lines are linear extrapolations of the measuring points between 0.5 and 2.5 mm chamber depth.

$$\dot{D}_t = s_{t,a} \frac{W}{e\, a\, \rho_o} k' \left(\frac{d(I\, k)}{dl}\right)_{BGC} \quad (6)$$

where

$$k' = k_{br}\, k_{ba}\, k_{ra}\, k_{wi},$$

$$k = k_{ad}\, k_{ab}\, k_{el}\, k_{in}\, k_{di}\, k_{pe}\, k_{ac}\, k_{de},$$

a is the effective collector area of the measuring volume of the extrapolation chamber (collecting volume)

ρ_o the air density at reference conditions

I the ionization current of the extrapolation chamber; the measured current of the extrapolation chamber is corrected for the polarity of the collecting voltage, the leakage current and the charge collection loss to obtain the ionization current

l the depth of the collecting volume

k_{br} the correction for bremsstrahlung from the beta source

k_{ba} the correction for the difference in backscatter between tissue and the material of the collecting electrode

k_{ra} the correction for radial non-uniformity of the beam, i.e. perpendicular to the beam axis

k_{wi} the correction for the scattering and stopping of beta rays by the entrance window

k_{ad} the correction for the deviation of the air density from ρ_o

k_{ab} the correction for the attenuation of the beta rays between the beta source and the entrance window

k_{el} the correction for the electrostatic attraction of the entrance foil due to the collecting voltage

k_{in} the correction for interface effects between the air in the collecting volume and the adjacent entrance window and collector area

k_{di} the correction for divergence of the beam

k_{pe} the correction for the perturbation of the beta radiation by the side walls of the ionization volume of the extrapolation chamber

k_{ac} the correction for the attenuation of the beta rays in the collecting volume

k_{de} the correction for the radioactive decay of the beta source

Reference conditions are designated as air temperature T_o = 293.15 K, air pressure p_o = 101.3 kPa and relative humidity 45 %.

The quantities and corrections appertaining to eq.(6) are discussed in detail in section 5. The symbols of the quantities and corrections considered are given in brackets after the title of every subsection. The effort to determine several corrections can be considerably reduced by restricting the range of chamber depths to 0.5 mm to 2.5 mm, because at larger chamber depths the deviations of the correction factors from unity become large and must be known more accurately. This is demon-

strated by figure 6 for the sources of types 1 to 3. Though the correction factors k_{ad}, k_{ab}, k_{el}, k_{in}, and k_{de} have already been considered for correcting the ionization current for all the chamber depths between 0.5 mm and 10.5 mm, the slope of the extrapolation curve is far from being constant, even for the type 1 source at chamber depths greater than 4 mm. Past experience has shown that the range of chamber depths from 0.5 mm to 2.5 mm is sufficient for the evaluation of all extrapolation curves.

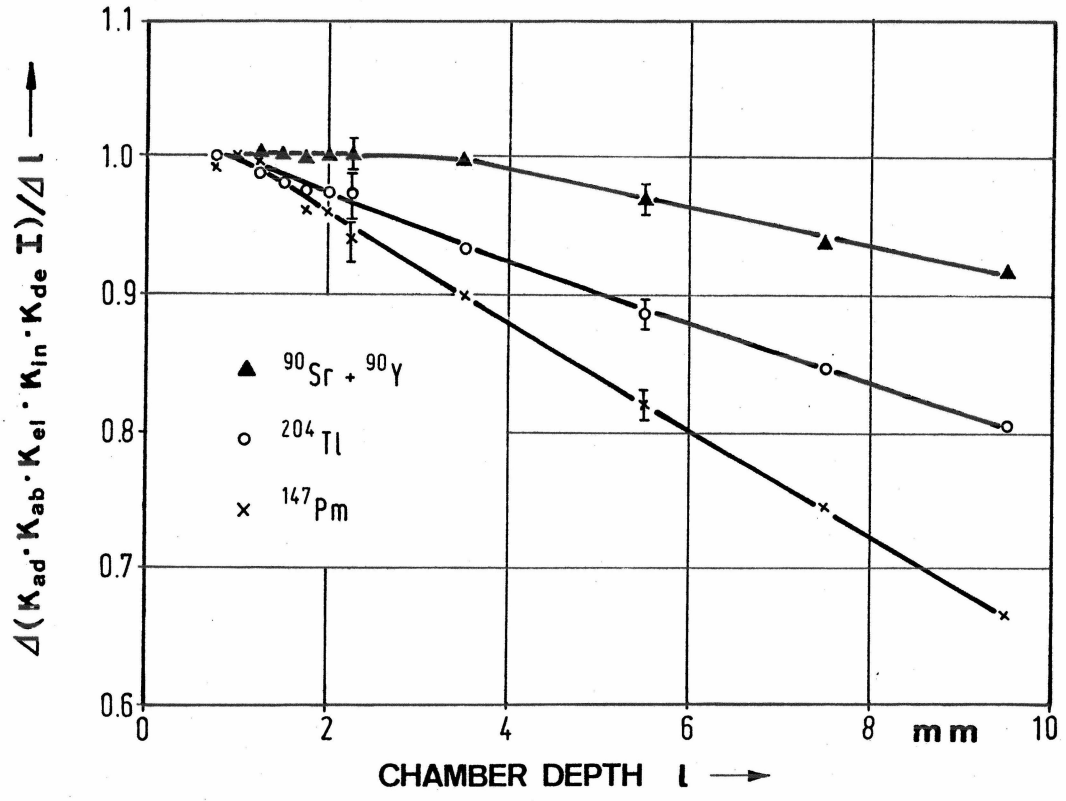

Figure 6: Slope of the extrapolation curves of sources of types 1 to 3 dependent on the chamber depth l. The correction factors k_{ad}, k_{ab}, k_{el}, k_{in}, and k_{de} are considered for correcting the ionization current I.

5. QUANTITIES AND CORRECTIONS APPERTAINING TO EQ.(6)

5.1 RATIO OF THE AVERAGE MASS COLLISION STOPPING POWERS ($s_{t,a}$)

The mass collision stopping power ratio $s_{t,a}$ was calculated for beta sources with the radionuclides (^{90}Sr + ^{90}Y), ^{204}Tl, and ^{147}Pm on the idealized assumption that the beta particles continuously dissipate their energy:

$$s_{t,a} = \frac{\int_0^{E_m} \Phi_E \, (S/\rho)_{col,t} \, dE}{\int_0^{E_m} \Phi_E \, (S/\rho)_{col,a} \, dE} \qquad (7)$$

where Φ_E is the relative spectral beta particle flux density in the collecting volume;

$(S/\rho)_{col}$ the mass collision stopping power for a beta particle of the kinetic energy E; additional index "t" for tissue and "a" for air;

E_m the maximum energy of the beta particles in the collecting volume.

Φ_E was measured at the calibration distance by uncooled 150 mm^2 and 200 mm^2 Si(Li) semiconductor detectors of 0.3 mm and 5 mm thickness and is shown in figure 7. These data for Φ_E not corrected for backscattering loss (backscatter factor below 1.1 for all radionuclides) and instrumental resolution can be used to calculate $s_{t,a}$ with sufficiently good approximation as $s_{t,a}$ depends only slightly on the beta particle energy. The most accurate data for $s_{t,a}$ based on the $(S/\rho)_{col}$

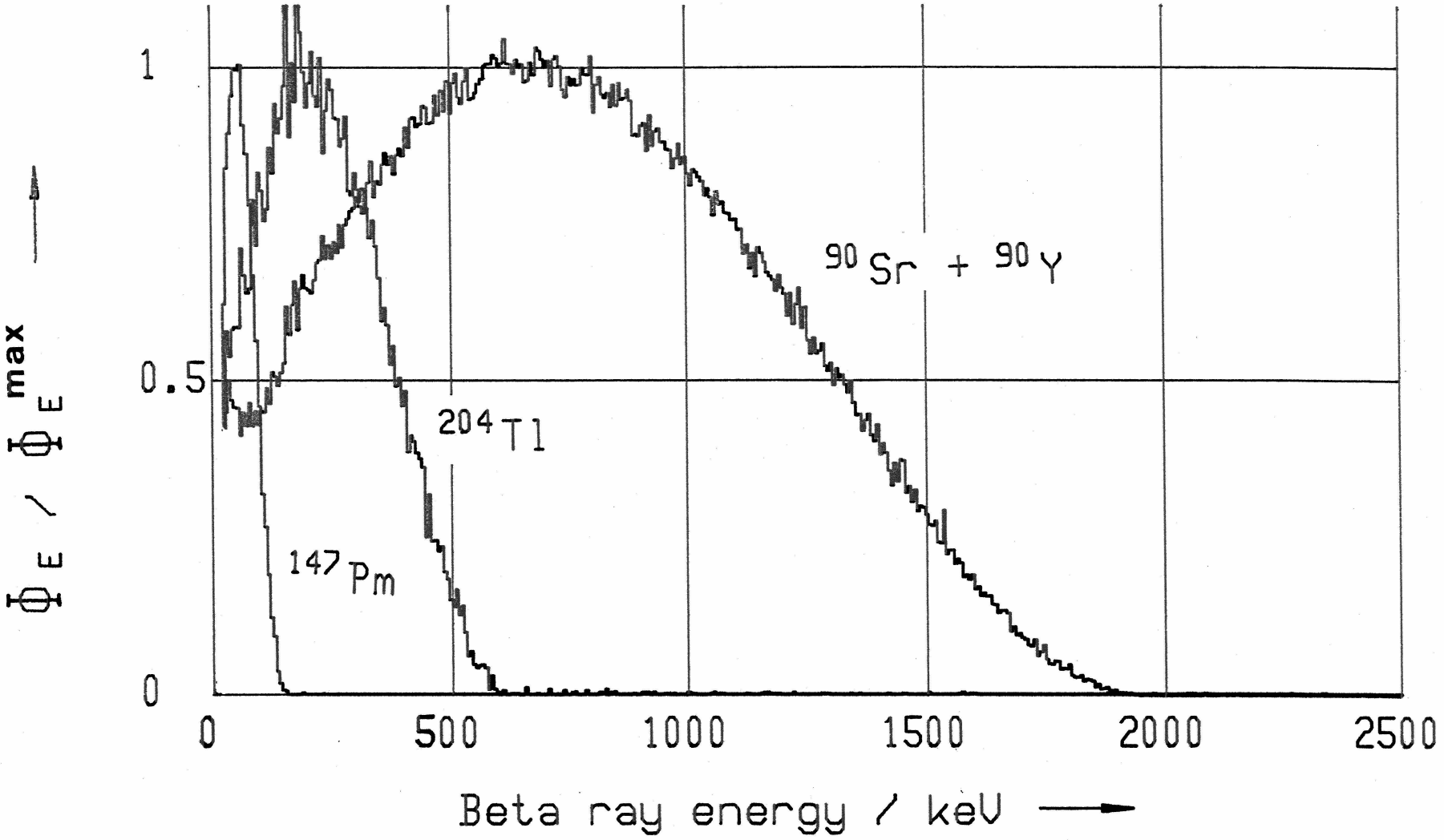

Figure 7: Relative spectral beta particle flux densities of sources of the radionuclides (^{90}Sr + ^{90}Y), ^{204}Tl, and ^{147}Pm with beam flattening filters (sources of types 1 to 3, see table 1). The flux densities are normalized to the same maximum value Φ_E^{max}, but not corrected for instrumental resolution or detector backscattering loss.

data of Seltzer /24/ are shown in the first line of table 2. Other $s_{t,a}$ values based on older $(S/\rho)_{col}$ data and calculated for a slightly different composition of soft tissue are shown in the 2nd and 3rd lines of table 2 for comparison. $s_{t,a}$ values used by Owen /16/ are given in the last line.

The $s_{t,a}$ values can be assumed to be equal for sources of the same radionuclides but of different types (see table 1). They do not even differ very much for the three different radionuclides.

Table 2: Calculated mass stopping power ratios $s_{t,a}$ for beta sources with the radionuclides (^{90}Sr + ^{90}Y), ^{204}Tl, and ^{147}Pm. u_{sy} is the estimated relative systematic uncertainty of $s_{t,a}$.

$(S/\rho)_{col}$ data taken from	Type of tissue	$s_{t,a}$ for			u_{sy} in %
		$^{90}Sr+^{90}Y$	^{204}Tl	^{147}Pm	
/24/ 1986	see p. 7	1.110	1.121	1.124	± 1.5
/25/ 1972	Muscle, striated (ICRU) see /26/	1.111	1.139	1.150	± 1.5
/26/ 1984		1.111	1.122	1.125	± 1.5
/27/ 1964, /28/ 1966		1.122	1.139	1.146	± 2.0

5.2 AVERAGE ENERGY REQUIRED TO PRODUCE AN ION PAIR IN AIR; ELEMENTARY CHARGE (W, e,)

The recommended conventional values of the average energy required to produce an ion pair in dry air, W, have increased during the last

decades (second column in table 1). The W/e value for laboratory air with a relative humidity of 45 % is obtained /29/ by multiplying the values for dry air with the factor 0.997 (third column in table 3) *).

Table 3: W for dry air and W/e for air with a relative humidity of 45 %.

Reference	W for dry air in eV	W/e for air of relative humidity 45 % in V
/22/ 1962	33.73 ± 0.15	33.63 ± 0.15
/30/ 1979	33.85 ± 0.15	33.75 ± 0.15
/31/ 1985	33.97 ± 0.06	33.87 ± 0.06

5.3 EFFECTIVE COLLECTOR AREA (a)

The effective collector area is defined as the quotient of the collecting volume and the chamber depth l and differs slightly from the geometric collector area generated by inscribing a circular groove (see figure 3) of the width x_g (= 0.2 mm) in the graphited surface (6) of the piston (see figure 2). A second groove with the same lathe setting was inscribed in a perspex dummy of the same dimensions as the graphited

*) The calibrations of the PTB secondary standards 1 to 65 are based on the older values of W (= 33.73 eV for dry air, see table 3), k_{ba} (= 1), and $s_{t,a}$ (see 2nd line of table 2). The $\dot{D}_t(0)$ values of the certificates should be multiplied by 1.016, 1.001, and 0.984 for the sources of the radionuclides (^{90}Sr + ^{90}Y), ^{204}Tl, and ^{147}Pm, respectively, to take into account the more recent values.

piston to measure the diameter x_a of the geometric collector area and the width x_g of the groove directly with a measuring microscope. Thus the sum $(x_a + x_g)$ regarded as the diameter of the effective collector area could be measured with a relative empirical standard deviation of single measurement of 0.1 % obtained from 4 measurements.

The potential difference between the collector area and the guard ring was always kept below 1 mV and is small compared with the collecting voltage. The distortion of the electric field of the collecting volume due to this potential difference /32/ could therefore be neglected. Blechschmidt's formula /33/ for a capacitor with plane parallel circular electrodes with a guard ring was used to calculate the chamber capacity C_k,

$$C_k = \varepsilon (x_a + x_g)^2 \pi / (4\, l), \qquad (8)$$

where ε is the dielectric constant. To calculate C_k with eq.(8) the chamber depth l had to be determined from the indication of the micrometer screw, considering the zero point of the chamber depth setting. The zero point was obtained by measuring C_k versus l and extrapolating C_k^{-1} to $l = 0$. The change of the zero point with the ambient temperature T of the extrapolation chamber was experimentally determined as $(-3.3 \pm 0.1)\ \mu m\ K^{-1}$ in the range $292\ K \leq T \leq 303\ K$.

The C_k values obtained with eq.(8) and by direct measurements with a measuring bridge agreed within $\pm$ 0.2 % in the range of $0.5\ mm \leq l \leq 2.5\ mm$ despite the unevenness of the collector shown in figure 4.

5.4 CORRECTION FOR THE AIR DENSITY IN THE COLLECTING VOLUME (ρ_o, k_{ad})

Every current measurement is referred to the air density ρ_o = 1.1995 kg m^{-3} at reference conditions (see page 20). The ionization

current must be multiplied by

$$k_{ad} = \frac{p_o\, T}{p\, T_o} \qquad (9)$$

to correct the air density under the conditions of the measurement (absolute temperature T, air pressure p) to reference conditions. The estimated relative systematic uncertainties of the quantities ρ_o, T, and p are $\pm$ 0.04 %, $\pm$ 0.03 %, and $\pm$ 0.02 %, respectively.

5.5 DETERMINATION OF THE IONIZATION CURRENT (I)

The current measured at the socket (8) of the extrapolation chamber (see figure 2) is composed of a number of component currents caused by

- the ionization of beta rays in the collecting volume. This current must be measured, the other component currents are regarded as disturbing ones.
- leakage of the chamber, not induced by pre-irradiation of the chamber. This current is about 0.01 fA (resolution of the current measuring system) for the type 1 extrapolation chamber and 1 fA for the type 2 extrapolation chamber. The leakage current varies only slowly with time, and can therefore easily be corrected for. The origin of the relatively high leakage current of the type 2 chamber has not yet been discovered.
- radiation induced leakage. This current is negligible if absorbed dose rates of beta sources with relatively low activity (< 40 MBq) positioned at relatively large distances from the chamber (> 20 cm) are measured. Otherwise, this current must be taken into account; for example, a current of 10 fA was measured after irradiating a type 1 chamber for several days with a (^{90}Sr + ^{90}Y) source of 4 GBq activity at a distance of 10 cm. This current decayed with a time constant of several weeks.

- the ionization of beta particles or of bremsstrahlung produced by the beta particles in the air of the preamplifier or in small air gaps in the close vicinity of the wire connecting the collecting electrode and the preamplifier. This ionization in the preamplifier can be neglected as the beta rays and bremsstrahlung are shielded by a perspex and an iron wall each 10 mm thick. The current originating in the air gaps is also assumed to be negligible due to the chamber construction.
- beta particles stopped in the perspex behind the collecting electrode (see figures 3 and 4) and diffusing to this electrode and the wire connecting this electrode with the socket (8). This negative current may be relatively large for the type 1 chamber (up to about 10 % of the current due to the ionization in the collecting volume) due to the thick perspex block behind the collector area. Measurements with this chamber show that the polarity current increases exponentially with a time constant of about one minute after the onset of irradiation. A 10 min pre-irradiation of the chamber was therefore performed each time to obtain a stable chamber current. After the end of the irradiation the current decreases with approximately the same time constant.

The negative current due to the electrons diffusing out of the perspex causes the "polarity effect" /34/ expressed as the deviation of the chamber current from the current due to ionization in the collecting volume, divided by the latter current. The magnitude of the polarity effect can be recognized from the saturation curves shown in figure 8 for an irradiation of the type 1 chamber with a (^{90}Sr + ^{90}Y) source at a distance of 30 cm. The saturation curves with their most satisfactorily flat plateaus do not exhibit mirror symmetry with respect to the abscissa. Mirror symmetry could be reached by shifting the abscissa to the chamber current -3.7 fA. Irrespective of the magnitude of the

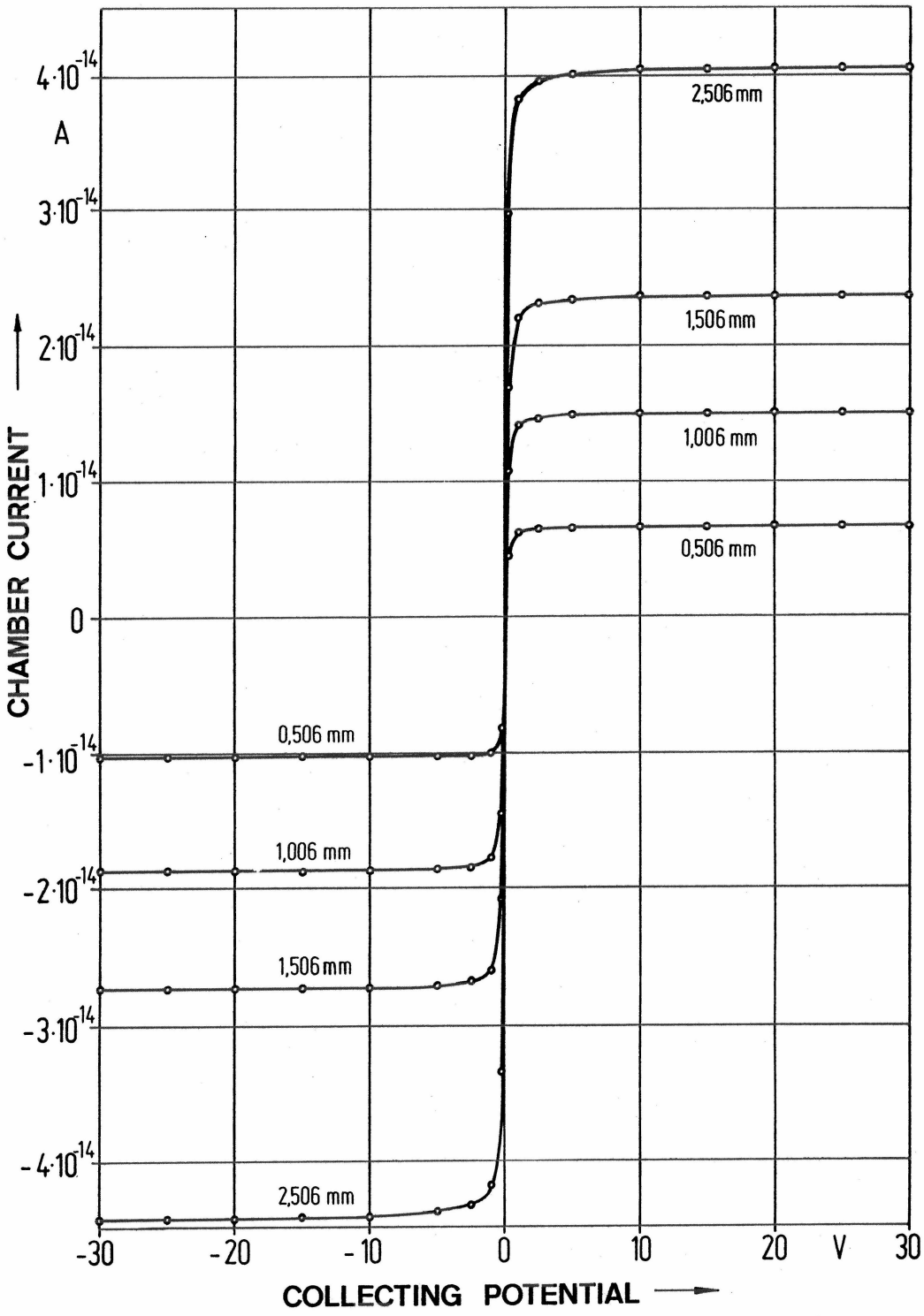

Figure 8: Saturation curves obtained with the type 1 extrapolation chamber irradiated with a source of type 1. The parameter is the chamber depth.

collecting potential U, the sum ($I_+ + I_-$) of the currents obtained for positive and negative polarity of U (I_- is negative!) yields the same value within the limits of uncertainty (figure 9).

The polarity effect of the type 2 chamber is small. It is between about 0.5 % and 2.4 % for chamber depths between 0.5 mm and 2.5 mm for an irradiation with a (^{90}Sr + ^{90}Y) source.

If the type 1 chamber is irradiated by a beta source, the negative "polarity current" is the only current to be measured in the limiting case of zero chamber depth independent of the polarity of the collecting potential. This is shown in figure 10 for the radionuclides (^{90}Sr + ^{90}Y), ^{204}Tl, and ^{147}Pm (sources of type 1 to 3, see table 1). The

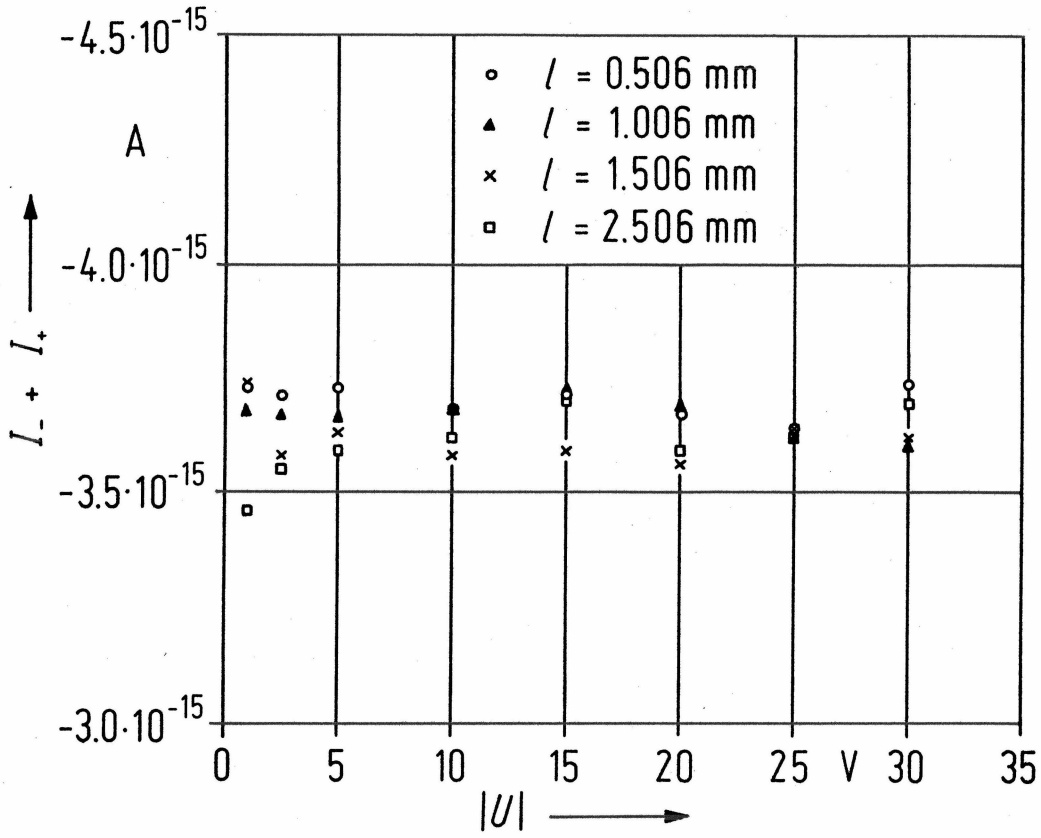

Figure 9: Sum of the chamber currents for a source of type 3 obtained at positive and negative polarity of the collecting voltage U.

chamber currents I_+ and I_- measured at positive and negative polarities of U are normalized by the current $I_-(l = 1.506$ mm) and extrapolated towards $l = 0$. The straight lines belonging to the same radionuclide intersect the ordinate for each radionuclide at the same point within the limits of uncertainty. The polarity effect is most pronounced for (^{90}Sr + ^{90}Y) with the highest mean energy of the beta particles.

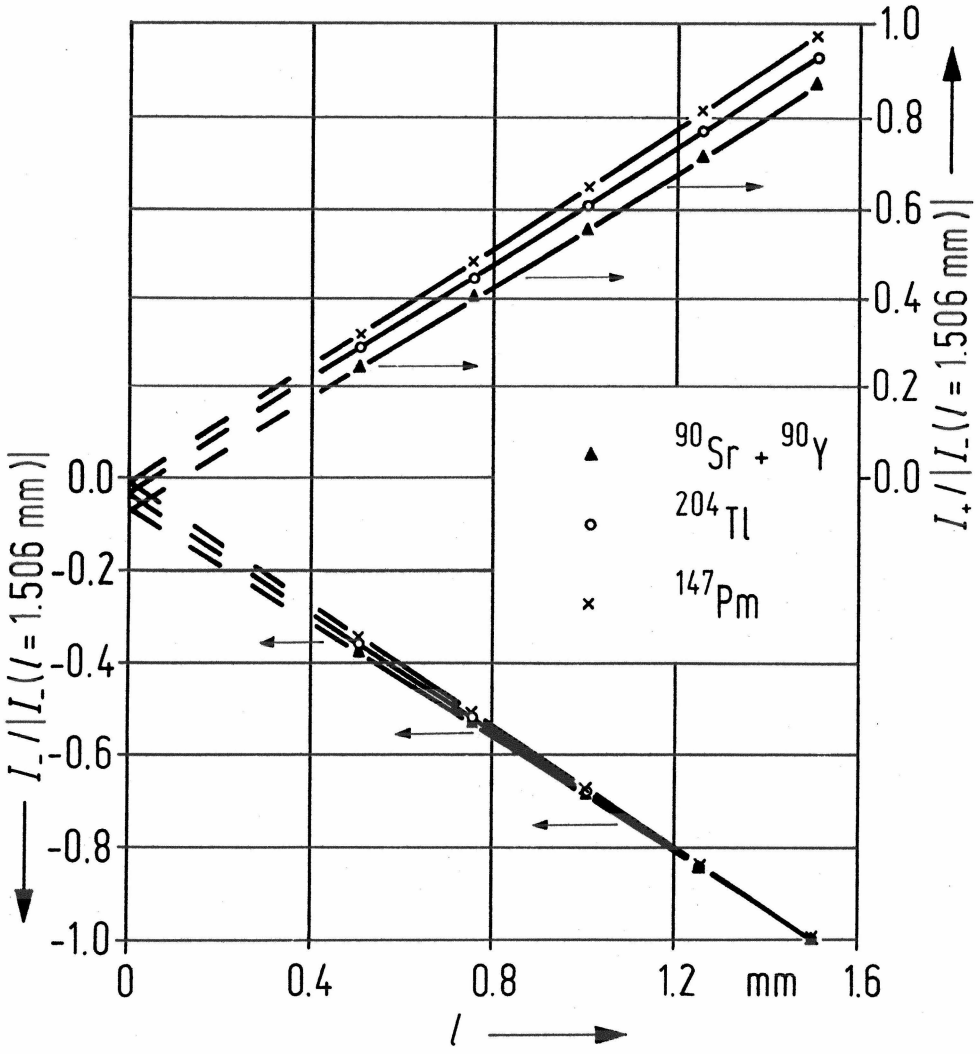

Figure 10: Extrapolation of the currents I_+ and I_- versus chamber depth $l = 0$ for sources of types 1 to 3 (see table 1).

The dependence of the magnitude of the polarity effect on the range of the beta particles also becomes apparent in the dependence of the polarity effect on the depth x in a soft tissue equivalent phantom. To demonstrate this, different absorbers were added in front of the entrance window and the currents I_+ and I_- were measured for the radionuclides (^{90}Sr + ^{90}Y), ^{204}Tl, and ^{147}Pm (sources of type 1 to 3, see table 1). The results are shown in figure 11. The polarity effect, expressed by the quotient $(I_- + I_+)/(I_- - I_+)$, decreases with phantom depth for (^{90}Sr + ^{90}Y) and ^{204}Tl, and is very small and almost constant for ^{147}Pm.

These measurements show that the polarity effect results in an additional negative current which does not depend on the magnitude and polarity of the collecting voltage and the chamber depth. This polarity current can be eliminated by measuring the currents I_+ and I_- at positive and negative voltage and subtracting one current from the other. The leakage current is thus also eliminated if it is constant during both measurements. The difference of I_+ and I_- is, on these assumptions, double the ionization current reduced due to lack of saturation resulting from volume recombination, initial recombination, and diffusion loss. The ionization current is determined by means of the collection efficiency f

$$I = (I_+ - I_-)/(2f) \tag{10}$$

and f is calculated by /35/:

$$f = (1 - \Gamma_o^2 \, l^4 \, q_m \, U^{-2})(1 - E_1 \, l \, U^{-1})(1 - 2 \, k^* \, T \, e^{-1} \, U^{-1}) \tag{11}$$

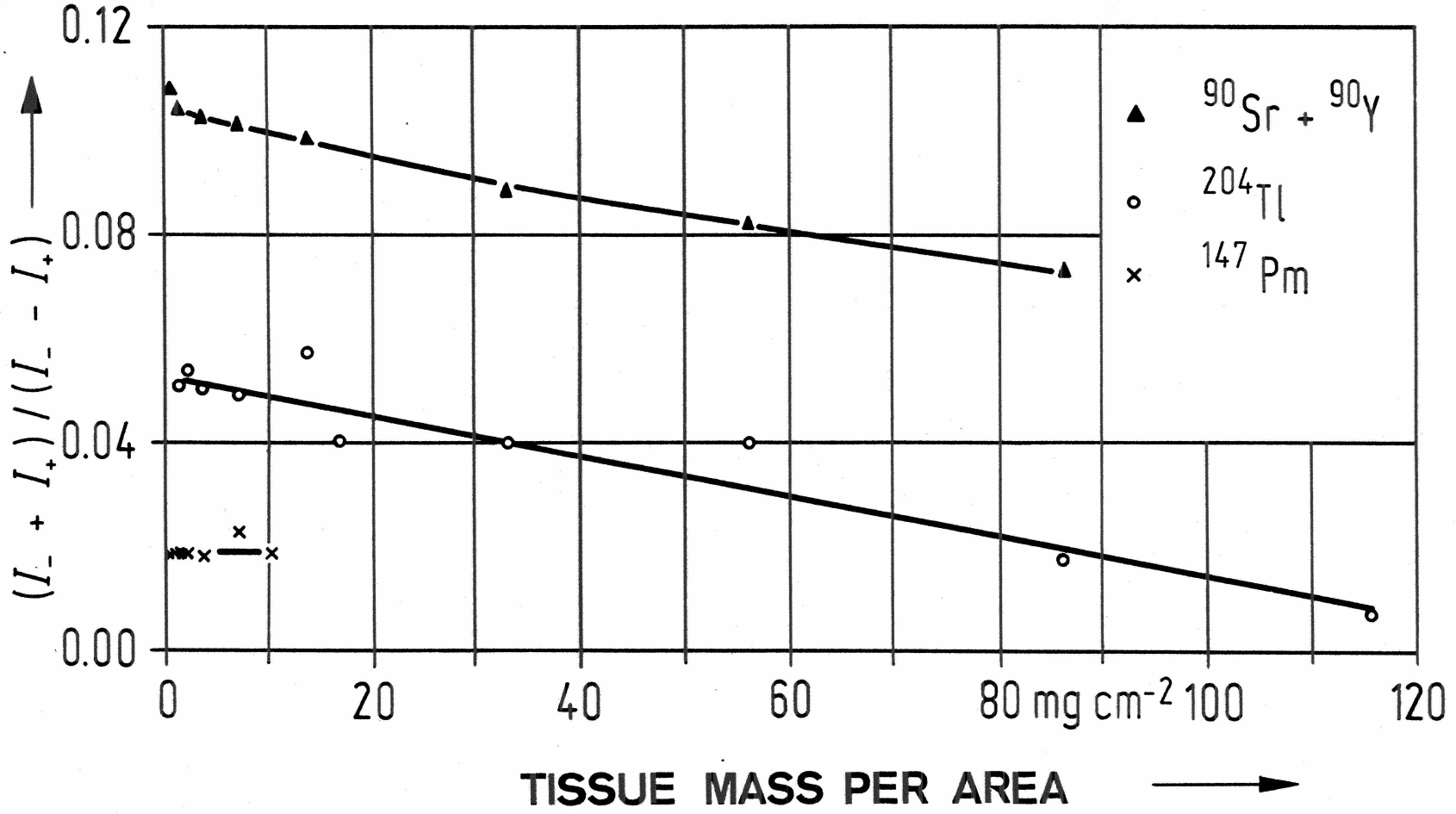

Figure 11: Dependence of the polarity effect, expressed by $(I_- + I_+)/(I_- - I_+)$, on the depth below the surface of the phantom, characterized as tissue mass per area, for sources of types 1 to 3 (see table 1).

where $\Gamma_o^2 = (5.05 \pm 0.25)\ 10^{13}\ V^2 A^{-1} m^{-1}$

l = chamber depth

q_m = measured ionization rate (collected charge per volume and time, $q_m = (I_+ - I_-)/(2al)$

a = effective collector area

U = collecting voltage (absolute value)

$E_1 = 4.4\ V\ m^{-1}$

e = elementary charge

T = air temperature

k^* = Boltzmann constant

$(2\ k^*\ T)/e = 0.0505\ V$ at $T = 293.15\ K$

The total estimated uncertainty of the charge collection loss (1-f) is lower than 10 % for f values above 0.98 which usually occur in practice.

5.6 CORRECTION FOR BREMSSTRAHLUNG FROM THE BETA SOURCE (k_{br})

In addition to that caused by beta radiation, a small part of the ionization current I is caused by bremsstrahlung emitted from the source. As the bremsstrahlung has a much greater penetrability than the beta radiation, the ionization current I_{br} due to bremsstrahlung can be measured by means of an absorber of low atomic number (perspex, Hostaphan) positioned in front of the entrance window of the extrapolation chamber just sufficiently thick to stop the beta radiation but only slightly attenuating the bremsstrahlung. The correction factor k_{br} for bremsstrahlung is defined by the equation

$$k_{br}\ I = I - I_{br}\ . \qquad (12)$$

Bremsstrahlung generated by the beta particles in the absorber can be neglected. Perspex absorbers 10 mm and 3.4 mm thick and a Hostaphan foil 0.25 mm thick were sufficient to stop the beta particles emitted from the sources of types 1 to 3 (see table 1) of the radionuclides (^{90}Sr + ^{90}Y), ^{204}Tl, and ^{147}Pm. k_{br} values between 0.994 and 0.999 ($\pm$ 0.002) have been determined for these sources at the surface of the phantom.

It has been demonstrated /36/, that the contribution of bremsstrahlung to the absorbed dose rate may be important if the calibration is not related to $\dot{D}_t(0)$ but to $\dot{D}_t(0.07)$, and the ratio $\dot{D}_t(0.07)/\dot{D}_t(0)$ is small. For example, the quotient of the exposure rate due to bremsstrahlung and the absorbed dose rate $\dot{D}_t(0.07)$ was experimentally determined as 1.7 R Gy^{-1} for a ^{147}Pm source of type 1 /36/. The corresponding quotient for $\dot{D}_t(0)$ instead of $\dot{D}_t(0.07)$ is higher by about a factor of 5. The effective energy of the bremsstrahlung photons is about 20 keV. The relatively low response (0.29) with respect to $\dot{D}_t(0.07)$ of a 0.39 mm thick TLD 100 thermoluminescence detector is changed for the ^{147}Pm source of type 1 by about 8 % due to bremsstrahlung.

5.7 CORRECTION FOR THE BACKSCATTER OF THE COLLECTING ELECTRODE AND GUARD RING (k_{ba})

Some of the incident beta particles are backscattered into the collecting volume by the collecting electrode and adjoining parts of the guard ring. Ideally, the beta particles should be backscatted in the same way as if the collecting electrode and the guard ring consisted of tissue, but as the collecting electrode consists of perspex alone for the type 1

and perspex and graphite for the type 2 extrapolation chamber, the difference in materials must be corrected for (correcting factor k_{ba}).

Measurements of backscatter factors B of perspex, graphite and the almost tissue-equivalent substance M3 /37/ relative to air were performed for secondary standard sources of the radionuclides (^{90}Sr + ^{90}Y) and ^{204}Tl by means of ultra thin $CaSO_4$:Dy/Teflon thermoluminescence dosemeters /38/. The backscatter factors were all equal (about 1.10) within the experimental uncertainty (variation coefficient 2 % obtained from 5 measurements). The experimentally determined backscatter factor for ^{147}Pm /11/ was much closer to unity (0.99).

The uncertainties of the experimentally determined backscatter factors are so large that small differences in the B values of materials with slightly different effective atomic numbers $\bar{Z}$ (definition of $\bar{Z}$ see /39/) could not be recognized. A small difference in the atomic numbers can be considered by assuming that, in first approximation, the absorbed dose rate due to backscattered radiation is proportional to $\bar{Z}$. This means that the backscatter factors B_t and B_p for tissue and perspex are related by

$$B_t = 1 + (B_p - 1)\,\bar{Z}_t/\bar{Z}_p\,, \qquad (13)$$

where $\bar{Z}_t = 6.50$ and $\bar{Z}_p = 5.85$ are the effective atomic numbers of tissue and perspex. The correction factor k_{ba} is given by

$$k_{ba} = B_t/B_p\,. \qquad (14)$$

The experimentally determined values of B_p and the values of k_{ba} calculated by means of the eqs. (13) and (14) are summarized in table 4. The relative systematic uncertainty of k_{ba} is much lower than that of B_p (about $\pm$ 2 %) because only the <u>difference</u> in backscatter of two

substances with only slightly differing $\bar{Z}$ values must be corrected.

Table 4: Backscatter factor B_p of perspex and correction factor k_{ba} obtained for sources of types 1 to 3 (table 1).

	Radionuclide		
	$^{90}Sr + ^{90}Y$	^{204}Tl	^{147}Pm
B_p	1.10	1.10	0.99
k_{ba}	1.010 ± 0.3 %	1.010 ± 0.3 %	1.000 ± 0.2 %

5.8 CORRECTION FOR THE NON-UNIFORMITY OF THE BEAM AT THE CALIBRATION DISTANCE (k_{ra}, k_{di}, k_{ac})

5.8.1 Radial non-uniformity

Because of the 30 mm diameter of the collector area, the absorbed dose rate is averaged over this area. If the absorbed dose rate has to be measured on the axis of the beam the non-uniformity perpendicular to the axis must be corrected for (correction factor k_{ra}). The non-uniformity can be measured e.g. by a photographic film /4/ or thermoluminescence detectors positioned perpendicular to the axis.

$k_{ra} = 1$ can be assumed if beam flattening filters according to the ISO standard /3/ are used.

5.8.2 Axial non-uniformity

Axial non-uniformity may be caused by the divergence of the beta rays (correction factor k_{di}) and their attenuation in the phantom (correction factor k_{ac}). The phantom is partly substituted by the extra-

polation chamber; at the point of interest the phantom material is replaced by the air of the collecting volume. The attenuation must therefore be considered for air instead of phantom material.

The absorbed dose rate in air, $\overline{\dot{D}_a}$, averaged over the collecting volume is calculated from $\dot{D}_a(y_o)$ at the entrance window by integration over the distance y from the source between y_o and y_o+l if the divergence is considered:

$$\overline{\dot{D}_a} = \int_{y_o}^{y_o+l} \dot{D}_a(y_o)\frac{y_o^2}{y^2}\,dy \Big/ \int_{y_o}^{y_o+l} dy = \dot{D}_a(y_o)\frac{y_o}{y_o+l} \qquad (15)$$

y_o is the distance from the source to the entrance window and l the chamber depth. As the entrance window is always positioned at a fixed distance of the phantom surface, k_{di} is obtained by

$$k_{di} = \dot{D}_a(y_o)/\overline{\dot{D}_a} = 1 + l/y_o. \qquad (16)$$

Attenuation of the beta rays by the air in the collecting volume need only be considered for beta rays of low energies, for example for ^{147}Pm sources. The air attenuation can be obtained, for example, from measurements of the attenuation of the beta rays by positioning Hostaphan foils in front of the entrance window (see section 5.14) and converting the results to air according to Cross /39/. For chamber depths below 2.5 mm

$$k_{ac} = 1 + c_{ac}\, l \qquad (17)$$

with c_{ac} of about 0.013 mm^{-1} was obtained for ^{147}Pm sources of type 1 (see table 1).

5.9 CORRECTION FOR THE AIR ATTENUATION OF THE BETA RAYS BETWEEN THE SOURCE AND THE SURFACE OF THE PHANTOM (k_{ab})

The lower the energy of the beta particles emitted from the source, the higher the probability that the beta particles are scattered or even stopped in the air between the source and the phantom surface. This probability depends on the air mass (proportional to the quotient of the air pressure p and the air temperature T) and its relative humidity r between the source and the phantom.

The dependence of $\dot{D}_t(0)$ on r, p, and T can be obtained by measuring the ionization current at a small chamber depth (e.g. 1 mm) for different values of r and p/T. Measurements showed that the correction for reference conditions can be neglected for sources of types 2 to 5 (see table 1). The correction factor k_{ab} taking into account the air attenuation can be written for ^{147}Pm sources of type 1 as

$$k_{ab} = c_1 \exp(c_2\, p/T) \exp(c_3\, r)\,, \qquad (18)$$

where the constants c_1 to c_3 may have the following values: c_1 = 0.00654; c_2 = 14.5 K kPa^{-1}; c_3 = 0.0437.

5.10 CORRECTION FOR THE RADIOACTIVE DECAY OF THE BETA SOURCES (k_{de})

The radioactive decay of the beta sources must be taken into account by the correction factor

$$k_{de} = \exp(\tau \ln 2/t_{1/2}), \qquad (19)$$

where $t_{1/2}$ is the half-life of the radionuclide and τ is the decay time to be corrected for. The following are examples of half-lives /43/:

$t_{1/2}$ = (10483 ± 110) days for (^{90}Sr + ^{90}Y),

$t_{1/2}$ = (1381 ± 8) days for ^{204}Tl,

$t_{1/2}$ = (957 ± 4) days for ^{147}Pm.

5.11 CORRECTION FOR THE ELECTROSTATIC ATTRACTION OF THE ENTRANCE WINDOW (k_{el})

The electrostatic attraction of the thin entrance window caused by the electric field in the collecting volume was determined by measuring the chamber capacity versus the collecting voltage at 2.5 mm chamber depth. An attraction of (2.2 ± 1.2) µm was measured at a field strength of 1000 V cm^{-1}. As all measurements were performed at field strengths ten times lower, the electrostatic attraction could be neglected and thus the correction factor $k_{el} = 1$ could be assumed.

5.12 CORRECTION DUE TO INTERFACE EFFECTS (k_{in})

The graphited perspex of the collector area and the graphited entrance window have somewhat lower effective atomic numbers than the air in the collecting volume. However, the disturbance of the secondary electron flux at these graphite-air interfaces can be neglected as can be deduced by measurements at a tin-air interface /40,41/, if the extrapolation chamber is operated in laboratory air at chamber depths larger than 0.5 mm. Thus the correction factor for interface effects is $k_{in} = 1$.

5.13 CORRECTION FOR THE PERTURBATION OF THE BETA PARTICLE FLUX DENSITY BY THE SIDE WALLS OF THE EXTRAPOLATION CHAMBER (k_{pe})

The perturbation of the beta particle flux density by the side walls of the extrapolation chamber has been studied in detail elsewhere /42/. The results show that the perturbation correction factor k_{pe} can be assumed to be the product of a shield factor and a scatter factor, the magnitudes of which depend on the chamber depth l. k_{pe} can be determined by measurements of the ionization current with rings of varying thickness and of the same inner diameter of the chamber. The rings are positioned in front of the entrance window. Examples of k_{pe} values used during the calibration of sources of types 1 to 3 are summarized in table 5.

Table 5: Perturbation correction factor k_{pe} for sources of types 1 to 3.

l in mm	Radionuclide		
	$^{90}Sr + ^{90}Y$	^{204}Tl	^{147}Pm
	Correction factor k_{pe}		
0.5	0.997	0.999	1.001
0.75	0.995	0.999	1.001
1.00	0.993	0.998	1.002
1.25	0.991	0.998	1.002
1.50	0.990	0.998	1.003
1.75	0.998	0.999	1.003
2.00	0.986	1.000	1.004
2.25	0.984	1.000	1.004
2.50	0.983	1.001	1.005

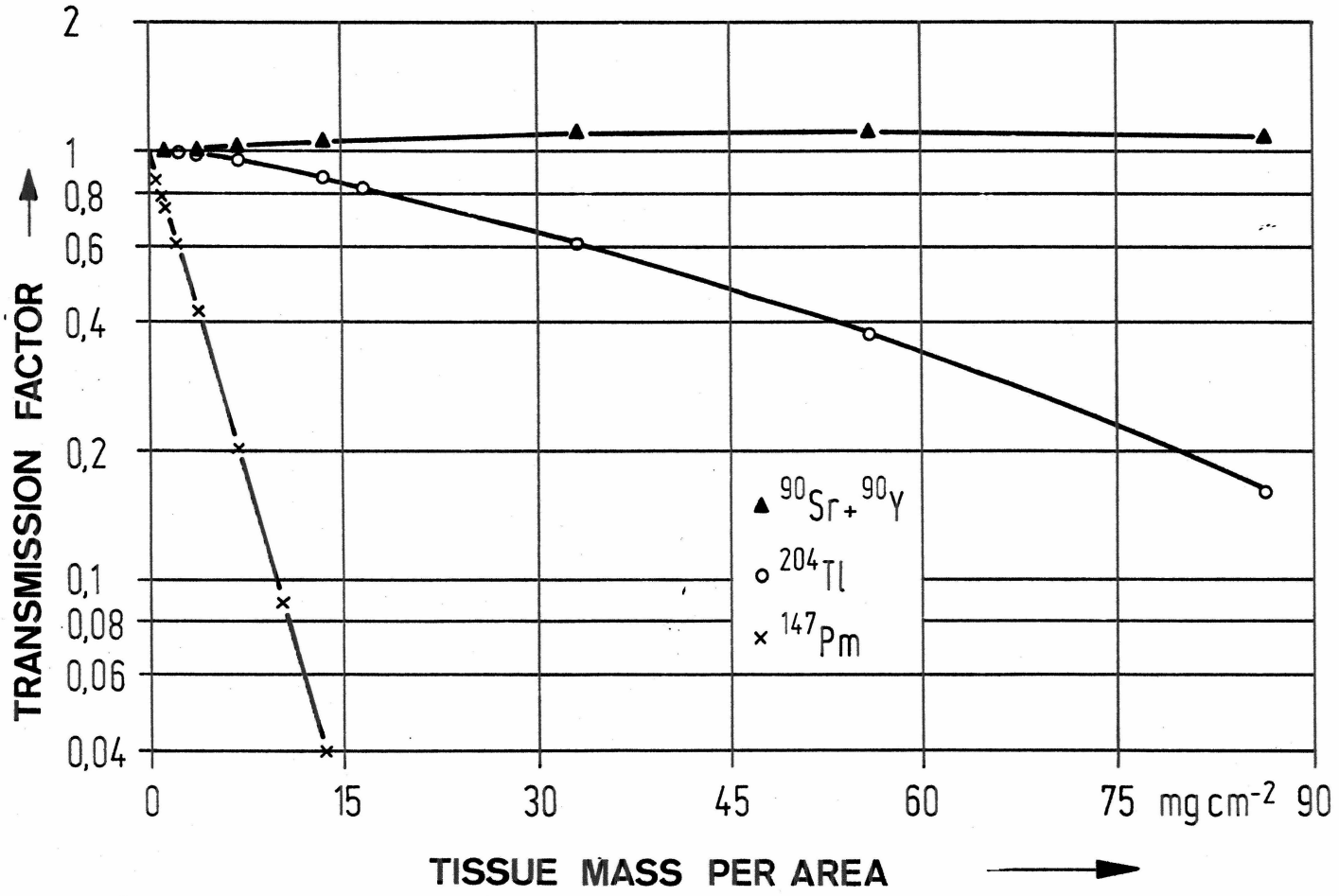

Figure 12: Transmission factors for sources of types 1 to 3 (see table 1).

5.14 CORRECTION FOR THE SCATTERING AND STOPPING OF BETA RAYS BY THE ENTRANCE WINDOW (k_{wi})

Depending on the energy of the beta particles, these may be stopped or more or less scattered by the thin thick entrance window of the extrapolation chamber. For example, the high-energy beta particles emitted from a (^{90}Sr + ^{90}Y) source of type 5 will only be scattered by the entrance window and thus give rise to a build-up of absorbed dose rate. On the other hand, a relatively large fraction of low-energy beta particles emitted from a ^{147}Pm source of type 1 is absorbed by the entrance window. The increase or decrease of the absorbed dose rate can be determined experimentally by placing Hostaphan foils or perspex absorbers of different thicknesses in front of the entrance window and measuring the ionization current I for a fixed chamber depth (e.g. l = 1 mm). The thickness of the absorbers can be determined by weighing them and measuring their areas. The mass per area values of Hostaphan are to be multiplied by 0.92 and those of perspex by 0.955 to obtain the tissue mass per area and thus the tissue depth x. The extrapolation of I(x) to x = 0 is performed by considering the respective functional dependence of I(x) in the vicinity of x = 0 for each source. For a (^{90}Sr + ^{90}Y) source of type 5 the current I(x) increases almost linearly with x for small x values, whereas I(x) decreases exponentially for a ^{147}Pm source of type 1. As long as the changes of the relative spectral beta particle flux densities with x do not markedly influence the $s_{t,a}$ value (see section 5.1), the quotient I(x)/I(0) can be regarded as the transmission factor T'(x). Examples of measured values of T'(x) are given in figure 12.

6 MEASUREMENT UNCERTAINTIES OF THE ABSORBED DOSE RATE TO TISSUE; NPL COMPARISON

The measurement uncertainty for $\dot{D}_t(0)$ obtained by the primary standard depends on the type and activity of the beta source and on the measuring distance from the source. Measurement uncertainties of the primary standard with the type 1 extrapolation chamber are stated in the following for sources of types 1 to 3 (see table 1) of an NPL secondary standard. The sources were measured eight times between 1974 and 1978: twice

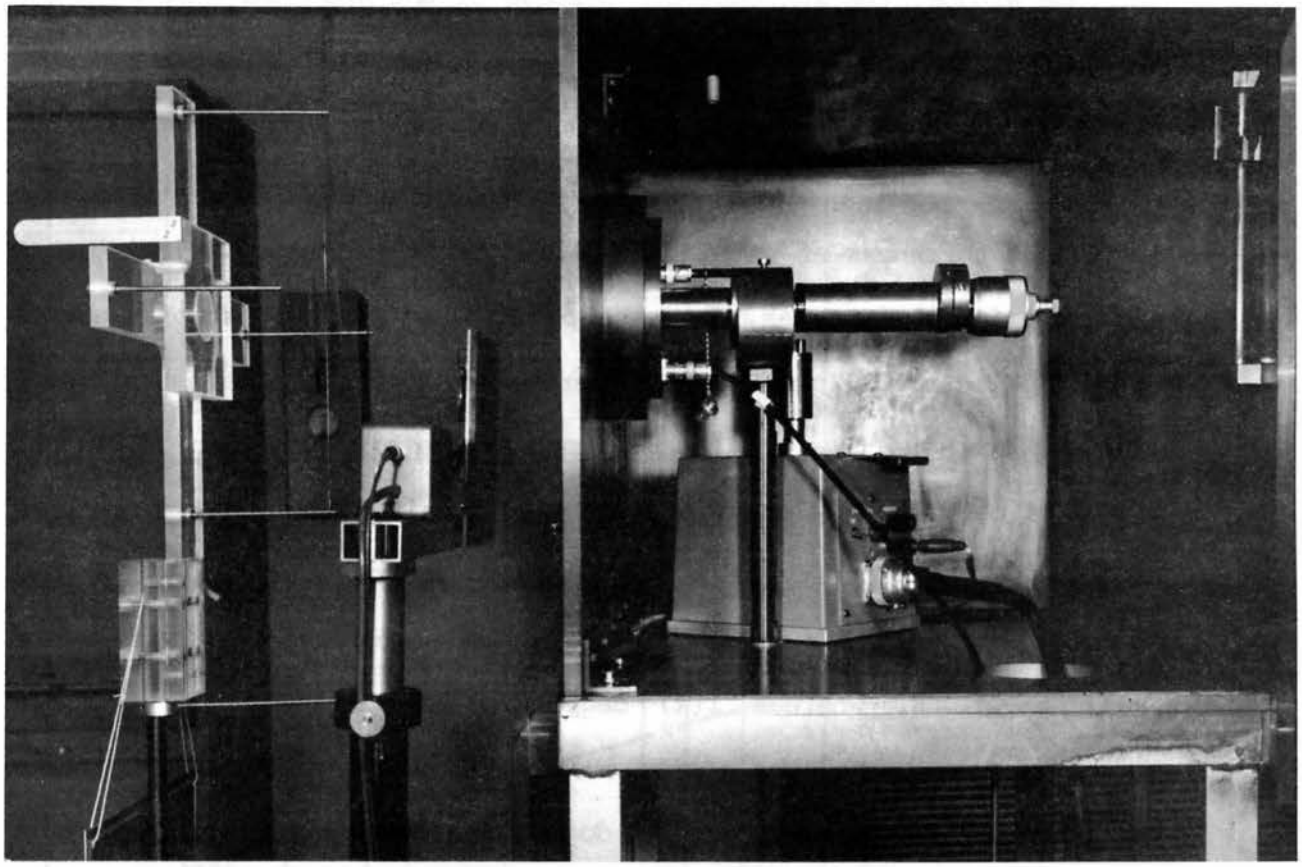

Figure 13: NPL jig with beta source and beam flattening filter (left) positioned in front of the type 1 extrapolation chamber (right). The extrapolation chamber is placed in a graphited grounded housing of perspex to avoid electrical disturbances and connected to the head of a vibrating capacitor amplifier.

for (^{90}Sr + ^{90}Y) (one source, no. 190), 3 times for ^{204}Tl (two sources, no. 390 and no. 407), and 3 times for ^{147}Pm (two sources, no. 590 and no. 607). Figure 13 shows a photograph of the jig of an NPL secondary standard positioned in front of the type 1 extrapolation chamber. The measurement conditions are listed in table 6.

Table 6: Measurement conditions during the intercomparison of types 1 to 3 sources at the PTB.

Chamber depth in mm	0.5 to 2.5
Chamber current in fA	4 to 160
Capacity of the integrator in pF	20.08
Output voltage change of the integrator in mV	90 to 850
Integration time in s	100 to 1000
Collecting potential in V	±5 to ±25
Air pressure in kPa	99.7 to 101
Air temperature in °C	19.7 to 20.3
Relative air humidity in %	40 to 50

The results are compared (reference date 1 August 1978) with those obtained by Owen with an extrapolation chamber of completely different design /10/. The electrodes of this chamber consist of thin graphited Melinex films which are strengthened at the corners and suspended under tension by fine wires in a light framework.

The PTB measurements carried out between 1974 and 1975 are based on evaluations of the extrapolation curves obtained with the sources no. 190, 390 and 590. The PTB results dated 1978 are traced back to measurements of extrapolation curves with PTB secondary standard sources with

the same characteristics as the NPL sources. Factors for the PTB sources were determined, relating the slope of the extrapolation curve and the ionization current at a specified chamber depth (1000 µm). The NPL sources were measured at this depth only, and the absorbed dose rates were calculated by means of the factor obtained from the PTB sources. The statistical uncertainty of the slopes of the extrapolation curves obtained for the NPL sources measured in August 1978 is slightly higher due to this procedure.

The quantities and corrections necessary for calculating $\dot{D}_t(0)$ (see eq.(6)) which do not depend on the chamber depth and do not vary during the measurement of the extrapolation curve are summarized in table 7 together with their uncertainties. The other corrections applied to the current $(I_+ - I_-)/2$ before calculating the slope $d(k\,I)/dl$ are given in table 8 together with their uncertainties. The slope and its uncertainty is given for each of the eight measurements in table 9. The uncertainties of the slopes are determined for a 95 % confidence interval of a regression line fitted through the measured points and is regarded as the combined uncertainty of all the random and systematic component uncertainties listed in table 8.

The eight NPL results of $\dot{D}_t(0)$ are systematically somewhat higher than those of the PTB given in table 9; the results differ by a factor of

1.004 for the type 1 source ($^{90}Sr + ^{90}Y$),

1.008 for the type 2 sources (^{204}Tl),

1.023 for the type 3 sources (^{147}Pm),

if the same W/e and $s_{t,a}$ values of table 7 are taken both by the PTB and the NPL.

Table 7: Values and uncertainties of the correction factors and quantities for calculating $\dot{D}_t(0)$ according to eq.(6) which do not depend on the chamber depth and do not vary during the measurement of the extrapolation curve. Sources of the same radionuclides have the same values and uncertainties of the correction factors and quantities with the exception of k_{wi} for the ^{147}Pm sources no. 590 and 607. The value of k_{wi} for the source no. 607 is given in brackets.

Correction factor or quantity	Unit	Type of uncert.	Radionuclide		
			$^{90}Sr+^{90}Y$	^{204}Tl	^{147}Pm
$s_{t,a}$	-	sy	1.110 ± 1.5 %	1.121 ± 1.5 %	1.124 ± 1.5 %
W/e	V	sy	33.87 ± 0.2 %		
a	cm^2	sy	7.243 ± 0.1 %		
ϱ_o	$kg\ m^{-3}$	sy	1.1995 ± 0.04 %		
k_{br}	-	sy	0.998 ± 0.1 %	0.994 ± 0.2 %	0.996 ± 0.2 %
k_{ba}	-	sy	1.010 ± 0.3 %	1.010 ± 0.3 %	1.000 ± 0.2 %
k_{ra}	-	sy	1.000 ± 0.2 %	1.000 ± 0.2 %	1.000 ± 0.5 %
k_{wi}	-	sy	0.997 ± 0.2 %	1.000 ± 0.2 %	1.145 (1.162) ± 1.5 %

Table 8: Values and relative uncertainties of the correction factors for calculating $\dot{D}_t(0)$ according to eq.(6) which depend on the chamber depth or may vary during the measurement of the extrapolation curve. k_{de} is given in addition in the last line. A number marked by * indicates the extreme value or the greatest relative uncertainty of a correction factor.

Correction factor	Unit	Type of uncert.	Radionuclide		
			$^{90}Sr+^{90}Y$	^{204}Tl	^{147}Pm
f^{-1}	-	sy	1.021* ± 0.2 %*		
k_{ad}	-	sy	1.030* ± 0.06 %*		
k_{ab}	-	sy	1.000 ± 0.0 %	1.000 ± 0.2 %	0.927* ± 1.0 %
k_{el}	-	sy	1.000 ± 0.1 %		
k_{in}	-	sy	1.000 ± 0.0 %		
k_{di}	-	sy	1.016* ± 0.1 %*		
k_{pe}	-	sy	0.992* ± 0.2 %*	0.998* ± 0.1 %	1.005* ± 0.2 %
k_{ac}	-	sy	1.000 ± 0.0 %		1.056* ± 1.0 %*
k_{de}	-	sy	0.913* ± 0.2 %*	0.522* ± 0.7 %*	0.391* ± 0.7 %*

Table 9: Values of the slope of the extrapolation curve with their random uncertainties for a 95 % confidence level (5 degrees of freedom); values of $\dot{D}_t(0)$ obtained by multiplying the slope with the quantities and correction factors according to eq.(6); $\dot{D}_t(0.07)$ is obtained by multipying $\dot{D}_t(0)$ by T'(0.07).

Correction factor or quantity	Unit	Type of uncertainty	Radionuclide							
			$^{90}Sr+^{90}Y$		^{204}Tl			^{147}Pm		
			Source number							
			190		390		407	590		607
			Date of measurement							
			5 Nov 74	3 Aug 78	10 Feb 75	3 Aug 78	3 Aug 78	10 Jan 75	2 Aug 78	2 Aug 78
$\left(\frac{d(I\,k)}{dl}\right)_{BGC}$	pA m^{-1}	st	17.06 ± 0.2 %	15.49 ± 0.5 %	10.46 ± 0.3 %	5.47 ± 0.7 %	19.59 ± 0.5 %	25.72 ± 0.5 %	9.95 ± 0.6 %	22.04 ± 0.6 %
$\dot{D}_t(0)$	μGy s^{-1}		0.6773	0.6736	0.2393	0.2402	0.860	0.5020	0.4977	1.119
T'(0.07)	-	sy	1.034 ± 0.3 %		0.965 ± 0.3 %			0.238 ± 5 %	0.241 ± 5 %	0.232 ± 5 %
$\dot{D}_t(0.07)$	μGy s^{-1}		0.7003	0.6965	0.2309	0.2318	0.830	0.119	0.120	0.260

The experimentally determined T'(0.07) values (see table 9) enable $\dot{D}_t(0.07)$ to be calculated:

$$\dot{D}_t(0.07) = T'(0.07)\, \dot{D}_t(0) \qquad (20)$$

The quotients of the measured NPL and PTB values of $\dot{D}_t(0.07)$ are:

0.997	for the sources of type 1 ($^{90}Sr + {}^{90}Y$),
0.994; 0.987	for the sources 390 and 407 of type 2 (^{204}Tl),
0.927; 0.952	for the sources 590 and 607 of type 3 (^{147}Pm).

The quadrature sums (square roots of the sum of squares) Σ_1 of the component relative uncertainties are calculated from the values given in tables 7 and 9 and from the relative uncertainty of k_{de} for every type of source and shown in table 10 together with the corresponding values of the NPL. The values of W/e and $s_{t,a}$ and their relative systematic uncertainties are assumed to be the same for the PTB and NPL. To better judge the differences between the results for $\dot{D}_t(0.07)$, the quadrature

---

Table 10: Quadrature sums Σ_1 and Σ_2 of the component systematic and random uncertainties for the measurand $\dot{D}_t(0.07)$ (see text).

Source type	Σ_1		Σ_2	
	PTB	NPL	PTB	NPL
1	1.7	3.2	0.7	2.4
2	1.8	3.3	0.9	2.5
3	5.5	6.5	5.3	6.2

sums Σ_2 are also calculated; these differ from Σ_1 only by the fact that the component systematic uncertainties of W/e and $s_{t,a}$ are assumed to be zero.

The eight measured values of $\dot{D}_t(0)$ and $\dot{D}_t(0.07)$ obtained by the PTB NPL agree within the claimed uncertainties. The somewhat larger uncertainties of the NPL are caused by the chamber construction optimized to measure the absorbed dose to air free in air and not in a tissue equivalent phantom. For example, a comparatively large ($\pm$2 %, /16/) relative systematic uncertainty of the collecting volume is therefore claimed for the NPL chamber.

7 ACKNOWLEDGEMENTS

The author is indebted to Mr. Neudecker for his help and cooperation in arranging the experimental set-up, and wishes to thank Dr. Klaus Geiger for his helpful comments.

That part of the work dealing with the comparison of the beta sources by the NPL and the PTB was sponsored by the COMMISSION OF THE EUROPEAN COMMUNITIES under a study contract no. 1161/2 - 80 L/V.

8 REFERENCES

/1/ Gesetz über Einheiten im Meßwesen. (Act about units of measurement); Bundesgesetzblatt Teil I Nr. 11, S. 409 (1985).

/2/ Verordnung über den Schutz vor Schäden durch ionisierende Strahlen (Strahlenschutzverordnung - StrlSchV). (Ordinance on Protection against Damage and Injuries caused by Ionizing Radiation); Bundesgesetzblatt Teil I Nr. 125, S. 2905 (1976).

/3/ Reference beta radiations for calibrating dosemeters and doserate-meters and for determining their response as a function of beta radiation energy. International Organization for Standardization. International Standard ISO 6980-1984 (E), 1984.

/4/ J. Böhm: Standardization and Calibration in Beta Dosimetry. Proc. of the International Beta Dosimetry Symposium held at Washington, D.C. February 15-18, 1983. Report NUREG/CP-0050 (Washington, D.C. 20555) 1984.

/5/ J. Böhm: Die Kalibrierung von Beta-Dosismeßgeräten und Betastrahlenquellen in der Physikalisch-Technischen Bundesanstalt. Kernforschungszentrum Karlsruhe Report KFK 2185 (1975), 31-35.

/6/ M. Ehrlich, J.S. Pruitt and C.G. Soares: Standard Beta-Particle and Monoenergetic Electron Sources for the Calibration of Beta-Radiation Protection Instrumentation. Report NUREG/CR-4266 NBSIR 85-3169 (1985), U.S. Nuclear Regulatory Commission, Washington, D.C. 20555.

/7/ J.S. Pruitt: The Effect of Altitude on Beta Ray Source Calibrations. Rad.Prot.Dos. 11 (1985) 151-157.

/8/ P. Christensen: Practical Beta Dosimetry in Radiation Protection. CEC-Report EUR 7365 EN (1982) 146-160.

/9/ L.V.E. Caldas: Algun Metodos de Calibracao e de Dosimetria da Radiacao Beta. Tese da Universidade de Sao Paulo (1980).

/10/ B. Owen: The Beta Calibration of Radiation Survey Instruments at Protection Levels. Phys.Med.Biol. 17 (1972) 175-186.

/11/ B. Owen: Factors for Converting Beta-Ray Dose Rates Measured in Air to Dose Rates in Tissue. Phys.Med.Biol. 18 (1973) 355-368.

/12/ J. Böhm: Sekundärnormal für die Energiedosis durch Betastrahlung in Gewebe. PTB-Jahresbericht 1978, 193-194.

/13/ J. Böhm: Exchange of Sources, Beam Flattening Filters and Jigs of a Secondary Standard for Absorbed Dose Rates of Beta Radiation. PTB-Mitteilungen (1986), in press.

/14/ J. Böhm, K. Hohlfeld and H. Reich: A Primary Standard for the Determination of Absorbed Dose in a Phantom for X-Rays Generated at Potentials of 7.5 to 30 kV. PTB-Mitteilungen 89 (1979) 163-172.

/15/ J. Böhm, P. Hillion and J.P. Simoen: Intercomparison of the PTB and LMRI Standards in Beta Dosimetry. Aspects fondamentaux et appliques de la dosimetrie. Proc. 8. Congres international de la

societe francaise de radioprotection, pp. 110-121, Saclay 23-26 mars 1976.

/16/ B. Owen: Comparison of the NPL and PTB Absorbed Dose Rate Standards for Beta Radiation at Protection Levels. Contract No 1161/1-80 L/V. NPL Report RS 57. November 1981.

/17/ W. Bernau, L. Breitenhuber und H. Sorantin: Beschreibung der Extrapolationskammer für die Absolutmessung der Energiedosisleistung von Betastrahlung und weicher Röntgenstrahlung. Bericht OEFZS BER. No. 4257 (1983), Österreichisches Forschungszentrum Seibersdorf.

/18/ Radiation Quantities and Units. International Commission on Radiological Units and Measurements. ICRU Report 33 (Washington D.C. 20014), 1984.

/19/ Determination of Dose Equivalents Resulting from External Radiation Sources. International Commission on Radiological Units and Measurements. ICRU Report 39 (Washington D.C. 20014), 1985.

/20/ J. Böhm: A Measuring and Calibration System for Currents down to 10^{-17}A. Atomkernenergie 27 (1976) 139-143.

/21/ J. Böhm: Review of Extrapolation Chamber Measurements of Beta Rays and Low Energy X-Rays. Rad.Prot.Dos. 1986, in press.

/22/ Physical Aspects of Irradiation. International Commission on Radiological Units and Measurements. ICRU Report 10b (Washington D.C. 20014), 1962.

/23/ T.E. Burlin: Cavity-Chamber Theory. In: Radiation Dosimetry, Vol. 1 (2. edition), edited by F.H. Attix and W. Roesch, Academic Press New York, San Francisco, London (1968) 331-392.

/24/ S.M. Seltzer, National Bureau of Standards, private communication 1986.

/25/ L. Pages, E. Bertel, H. Joffre and L. Sklavenitis: Energy Loss, Range, and Bremsstrahlung Yield for 10-keV to 100-MeV Electrons. Atomic Data 4 (1972).

/26/ Stopping Powers for Electrons and Positrons. International Commission on Radiological Units and Measurements. ICRU Report 37 (Washington D.C. 20014), 1984.

/27/ M.J. Berger and S.M. Seltzer: Tables of Energy Losses and Ranges of Electrons and Positrons. NASA Publication SP-3012 (National Aeronautics and Space Administration, Washington), 1964.

/28/ M.J. Berger and S.M. Seltzer: Additional Stopping Power and Range Tables for Protons, Mesons and Electrons. NASA Publication SP-3036 (National Aeronautics and Space Administration, Washington), 1966.

/29/ J.-P. Guiho, I. Pavlicsek, A. Ostrowsky and H. Goenvec: Ionisation des gaz.- Influence de l'etat hygrometrique de l'air sur l'ionisation produite par les rayonnements X ou . C. R. Acad. Sc. Paris, Serie B (1974) 69-71.

/30/ Average Energy Required to Produce an Ion Pair. International Commission on Radiological Units and Measurements. ICRU Report 31 (Washington D.C. 20014), 1979.

/31/ CCEMRI, Section I, Paris, 8. Meeting, April 1985.

/32/ J.W. Boag: Distortion of the Electric Field in an Ionization Chamber due to a Difference in Potential between Guard Ring and Collector. Phys.Med.Biol. 9 (1964) 25-32.

/33/ E. Blechschmidt: Präzisionsmessungen von Kapazitäten, Induktivitäten und Zeitkonstanten, 2. Auflage. F. Vieweg & Sohn Verlag, Braunschweig (1956).

/34/ B. Markus: Ionization Chambers, Free of Polarity Effects, Intended for Electron Dosimetry. In: Dosimetry in Agriculture, Industry, Biology and Medicine. Proc.Ser. STI/PUB/311, IAEA (1973) 463-472.

/35/ J. Böhm: Saturation Corrections for Plane-Parallel Ionization Chambers. Phys. Med. Biol. 21 (1976) 754-759.

/36/ H. Schüren und M. Heinzelmann: Abschätzung des Photoneneinflusses bei Kalibrierungen am Sekundärnormal für Betastrahlung. Laborbericht D 2/80 der KFA Jülich GmbH (1980).

/37/ B. Markus: Über den Begriff der Gewebeäquivalenz und einige "wasserähnliche" Phantomsubstanzen für Quanten von 10 keV bis 100 MeV sowie schnelle Elektronen. Strahlentherapie 101 (1956) 111-131.

/38/ B.K.S. Murthy and J. Böhm: Measurements of Backscatter and Transmission Factors for Beta Rays Using Thermoluminescence Dosimeters. Rad.Prot.Dos. 2 (1982) 63-67.

/39/ W.C. Cross: Variation of Beta Dose Attenuation in Different Media. Phys.Med.Biol. 13 (1968) 611-618.

/40/ M. Schneider, J. Böhm, K. Hohlfeld, H. Reich: Experimental Determination of the Ion Dose in the Vicinity of Tin-Air Interface. Proc. 7th Symposium on Microdosimetry, 8.-12. Sept. 1980, Oxford/UK, pp. 231-241; Ed. J. Booz, H.G. Ebert, H.D. Hartfiel, EUR 7147 DE-EN-FR; Harwood Academic Publishers, Chur-London-New York 1981.

/41/ J. Böhm und M. Schneider: Determination of Absorbed Dose Rates with Air-Filled Extrapolation Chambers at Small Chamber Dimensions or Low Gas Pressures. CEC-Report EUR 7365 EN (1982) 190-197.

/42/ J. Böhm: The Perturbation Correction Factor of Ionization Chambers in ß-Radiation Fields. Phys. Med. Biol. 25 (1980) 65-75.

/43/ K. Debertin, Physikalisch-Technische Bundesanstalt Braunschweig, private communication, 1986.

/44/ International Vocabulary of Basic and General Terms in Metrology. Beuth Verlag Berlin/Köln 1984.